

Ultrastructure and phylogeny of *Parvodinium cunningtonii* comb. nov. (syn. *Peridiniopsis cunningtonii*) and description of *P. cunningtonii* var. *inerme* var. nov. (Peridiniopsidaceae, Dinophyceae)

Mariana S. Pandeirada^{a,b}, Sandra C. Craveiro^{a,b,*}, Niels Daugbjerg^c, Øjvind Moestrup^c, António J. Calado^{a,b}

^a Department of Biology, University of Aveiro, P-3810-193 Aveiro, Portugal

^b GeoBioTec Research Unit, University of Aveiro, P-3810-193 Aveiro, Portugal

^c Marine Biological Section, Department of Biology, University of Copenhagen, Universitetsparken 4, DK-2100 Copenhagen Ø, Denmark

Received 20 July 2022; revised 1 September 2022; accepted in revised form 7 September 2022; Available online 13 September 2022

Abstract

Two strains of peridinioids were isolated from a flooded stream near Aveiro, central Portugal, and examined by light microscopy, scanning electron microscopy and serial-section transmission electron microscopy. The two strains showed the same tabulation and cell shape as *Peridiniopsis cunningtonii*. One of the strains had lightly reticulated plates and spines in most hypothecal plates, matching the features of typical *P. cunningtonii*. The other strain showed smooth plates and consistently lacked spines in the apiculate hypotheca. The strains were similar in fine structure and had a central pyrenoid with a starch sheath and perforated by cytoplasmic channels. Details of the flagellar apparatus matched those known from *Parvodinium*, as did the remarkably long microtubular strand leading to an extruded peduncle that was visible in serial sections. Phylogenetic analyses based on partial LSU rDNA and the concatenated ribosomal operon placed the strain with the smooth hypotheca in a clade with *Parvodinium* species. The two strains grouped as closely related sister taxa in the partial LSU rDNA phylogeny. A new combination is proposed, *Parvodinium cunningtonii* comb. nov. and a new variety, *Parvodinium cunningtonii* var. *inerme* var. nov., is described.

© 2022 The Author(s). Published by Elsevier GmbH. This is an open access article under the CC BY-NC-ND license (<http://creativecommons.org/licenses/by-nc-nd/4.0/>).

Keywords: Dinoflagellates; Flagellar apparatus; Microtubular strand of the peduncle (MSP); SSU-ITS-LSU rDNA; *Peridiniopsis*; Pusule

Introduction

The genus *Peridiniopsis* Lemmermann, as currently circumscribed in the most recent flora on freshwater dinoflagellates, is recognized as polyphyletic (Moestrup and Calado 2018). Fifteen species of *Peridiniopsis* are recognized in the

flora, which are set apart from other peridinin-containing peridinioids by having a combination of six cingular plates and zero or one intercalary plates in the epitheca (Moestrup and Calado 2018). The general plate formula given for *Peridiniopsis* in Moestrup and Calado (2018) is po, x, 3–5', 0–1a, 6–7'', 6c, 4–6s, 5''', 2'''''. This formula allows for different combinations of numbers in different plate series and

*Corresponding author.

E-mail address: scraveiro@ua.pt (S.C. Craveiro).

provides a practical but artificial means of classification of the group. As an example, molecular-based phylogenies recently revealed that the common freshwater species previously known as *Peridiniopsis elpatiewskyi* (Ostenfeld) Bourrelly, which has no anterior intercalary plates, is a member of *Parvodinium* Carty (Kretschmann et al. 2019). With the transfer of *P. elpatiewskyi* to the genus *Parvodinium* the circumscription of that genus has stretched to include species without intercalary plates, in contrast to the presence of two anterior intercalary plates in all its previously recognized species (Carty 2008; Kretschmann et al. 2019; Moestrup and Calado 2018). Both *Parvodinium* and *Peridiniopsis* are currently assigned to the Peridiniopsidaceae, a monophyletic family that also includes the freshwater genus *Palatinus* Craveiro, Calado, Daugbjerg & Moestrup and the marine genus *Joshia* Z. Luo, Na Wang, K.N. Mertens & H. Gu (Gottschling et al. 2017; Luo et al. 2020; Pandeirada et al. 2022). An additional species, the marine dinoflagellate currently designated '*Scrippsiella*' *hexapraecingula* because of its three anterior intercalary plates, has also been shown to be a close relative of species of Peridiniopsidaceae; reinvestigation of this species may perhaps reveal a new genus of this family (Horiguchi and Chihara 1983; Luo et al. 2020).

In the original description of the Peridiniopsidaceae, the combined presence of six cingular plates and up to two intercalary plates in the epitheca were two of the main features considered to discriminate members of this family from members of the Peridiniaceae (Gottschling et al. 2017). The internal cell features of the Peridiniopsidaceae were summarized by Pandeirada et al. (2022) based on detailed fine structure descriptions available for several members of the family. This included *Peridiniopsis borgei* Lemmermann (the type species of *Peridiniopsis*), *Palatinus apiculatus* (Ehrenberg) Craveiro, Calado, Daugbjerg & Moestrup (the type of *Palatinus*) and a species of the complex *Parvodinium umbonatum*–*P. inconspicuum* (which includes the type of *Parvodinium*; hereafter designated *P. umbonatum*–*inconspicuum*); and was complemented with more limited information available from *Joshia chumphonensis* Z. Luo, Na Wang, K.N. Mertens & H. Gu, *Parvodinium parvulum* (Woloszyńska) Na Wang, K.N. Mertens & H. Gu and '*Scrippsiella*' *hexapraecingula* (Calado and Moestrup 2002; Craveiro et al. 2009; Horiguchi and Chihara 1983; Luo et al. 2020; Pandeirada et al. 2022). The currently known ultrastructural features of the Peridiniopsidaceae may be summarized as follows: the eyespot is of type A (with several layers of carotenoid-rich globules included in a chloroplast lobe) or B (like type A but covered on the sulcus side by a layer of vesicles with crystalloid contents); the chloroplast lobes often show thylakoid-free areas and are arranged in an extensive radial network, usually extending from a large central pyrenoid (which is sometimes penetrated by cytoplasmic channels), surrounded or not by starch; an apical pore complex is usually present with

an underlying apical fibrous complex (absent in *Palatinus*); an extruded peduncle is often present (visible in TEM; absent in *Palatinus*); an extensive, internally divided microtubular strand of the peduncle (MSP) is often present and extends to the peduncle (reduced and not reaching the cell surface in *Palatinus*); the pusule is variable, with different combinations of flat vesicles, cylindroid tubes and ramifying flat and tubular vesicles, with or without sac pusules; the basal bodies form an angle of 80–90°, each basal body associated with two microtubular roots; a layered connective (LC) links the dorsal side of the longitudinal microtubular root (root 1; LMR/r1) with the proximal posterior side of the transverse basal body (TB) and with a transverse striated root; the proximal end of the LMR/r1 connects, by two or three small fibres, to two or three triplets of the TB; the right-hand side of the longitudinal basal body (LB) associates with a single microtubule (single-stranded microtubular root; SMR/r2); the transverse microtubular root (root 3; TMR/r3) nucleates variable numbers of microtubules (the microtubular extension of the TMR; TMRE/r3E) with variable paths and sometimes associated with fibrous material (forming a circle with a fibrous core in *P. borgei*); the proximal ends of the two basal bodies are usually not directly linked by a fibre (present only in *Palatinus*); the exit points of both flagella and peduncle are surrounded by prominent striated collars that are usually connected to one another by striated fibres (Pandeirada et al. 2022).

Here we report on the external morphology and fine structure of two slightly different strains of peridinioids isolated from a flooded area of a stream located near Aveiro, central Portugal, both matching in shape and tabulation *Peridiniopsis cunningtonii* Lemmermann. Phylogenetic analyses based on rRNA gene sequences revealed that both these strains are closely related to *Parvodinium* species. A new combination in *Parvodinium* is proposed and a new variety described.

Material and methods

Biological material

Two cultures of dinoflagellates, preliminarily identifiable as *Peridiniopsis cunningtonii*, were started from cells isolated from plankton samples collected in Ribeiro da Palha (40°33.240'N, 8°34.095'W), a flooded stream near the village of Nariz, Aveiro, Portugal, on two different dates. One culture line, *P. cunningtonii* strain 1, was started from a single cell isolated into MBL culture medium (Nichols 1973) from a sample collected on 16 July 2015. Cells from strain 1 had the plate tabulation of *Peridiniopsis cunningtonii* but did not have the hypothecal spines characteristic of typical *P. cunningtonii*. A second culture line, *P. cunningtonii* strain 2, was started from a single cell, isolated from a sample collected on 17 October 2016, into quadruple concentration L16 medium supplemented with vitamins

(Lindström 1991; Popovský and Pfister 1990). Cells of strain 2 came from a field population that displayed the plate tabulation and hypothecal spines characteristic of typical *P. cunningtonii*, and cultured cells maintained these features until the culture was lost six months later. Both cultures were kept at 18°C and a 12:12 light:dark photoperiod with a photon flux density of ca. 25 $\mu\text{mol m}^{-2} \text{s}^{-1}$.

Light microscopy (LM)

Photographs were taken with a Zeiss Axioplan 2 imaging light microscope (Zeiss, Oberkochen, Germany) equipped with DP70 or ColorView IIIu Olympus cameras (Olympus, Tokyo, Japan). Cell division in *P. cunningtonii* strain 1 was recorded with a JVC TK-C1481BEG colour video camera (Norbain SD, Reading, UK) mounted on a Leitz Labovert FS inverted light microscope (Leica Microsystems, Wetzlar, Germany).

Scanning electron microscopy (SEM)

Three fixation protocols were used to observe different aspects of motile cells of *P. cunningtonii* strain 1. For clear observation of amphiesmal plates, cells were fixed by 1) mixing equal volumes of culture and ethanol 50 %, for 40 min and 2) by mixing 0.95 ml of culture and 0.05 ml 2 % aqueous OsO_4 , for 5 min. Cells with the flagella in situ were obtained by fixing 3) a mixture of two volumes of culture and one volume of a 3:1 (v/v) mixture of aqueous 2 % OsO_4 and saturated HgCl_2 , for 1 h. Fixed cells from all fixation protocols were retained on Nuclepore polycarbonate filters with 5- μm pore size (Whatman, GE Healthcare Life Sciences, Maidstone, UK). Filters from fixations 2 and 3 were washed with distilled water for 30–45 min before dehydration in a graded ethanol series, together with filters from fixation 1. The dehydrated filters were critical-point-dried in a Baltec CPD-030 (Balzers, Liechtenstein), glued onto stubs and sputter-coated with gold–palladium. Cells were observed in the scanning electron microscopes Hitachi S-4100 (Hitachi High-Technologies, Tokyo, Japan) and JEOL JSM 6335F (Jeol, Tokyo, Japan).

Transmission electron microscopy (TEM)

Swimming cells from both cultures were fixed for 40–75 min in 2 % glutaraldehyde made in phosphate buffer 0.1 M, pH 7.2 (final concentration). In addition, swimming cells from the culture of *P. cunningtonii* strain 2 were fixed in a mixture of 1 % glutaraldehyde and 0.5 % OsO_4 (final concentrations) in phosphate buffer 0.1 M, pH 7.2, for 25 min. The fixed cells were washed in phosphate buffer, included into 1.5 % agar blocks, and post-fixed with 0.5 % or 1 % OsO_4 (final concentrations) in the same buffer. After being washed in phosphate buffer and distilled water, the blocks were dehydrated through a graded ethanol series

and propylene oxide, and embedded in low viscosity resin (Agar Scientific, Stansted, Essex, UK). The blocks were sectioned with an EM UC6 ultramicrotome (Leica Microsystems, Wetzlar, Germany). Ribbons of serial sections (70 nm thick) were transferred with slot grids to Formvar film and stained with uranyl acetate and lead citrate. Sections of three cells of *P. cunningtonii* strain 2 and three cells of strain 1 were observed in a JEM 1010 electron microscope (JEOL, Tokyo, Japan), equipped with a Gatan Orius digital camera (Gatan Inc., Pleasanton, California, USA).

Single-cell PCR amplification of LSU rDNA

Seven swimming cells from culture of *P. cunningtonii* strain 1 were isolated into one 0.2-ml PCR tube and frozen at -8°C for 2 days. PCR amplification of partial LSU rDNA involved external primers D1R (Scholin et al. 1994) and 28-1483R (Daugbjerg et al. 2000), and a bead of illustra™ puReTaq Ready-To-Go PCR Beads kit (GE Healthcare, UK). The reaction was conducted in a thermocycler Biometra-Tprofessional (Biometra GmbH, Göttingen, Germany), with thermal profile as in Pandeirada et al. (2014). The amount of amplified LSU rDNA was increased through nested PCR using 2 μl of the first PCR products and two primer combinations: D1R with D3A and D3B with 28-1483R. The thermal profile was the same as in Pandeirada et al. (2017). The nested-PCR products were purified using the QIAquick PCR Purification Kit (Qiagen, Hilden, Germany), and sent to Macrogen Europe (Amsterdam, Netherlands) for sequence determination with primers D1R, D2C, D3A, D3B and 28-1483R (Daugbjerg et al. 2000; Nunn et al. 1996; Scholin et al. 1994).

DNA extraction and PCR amplifications of SSU rDNA, ITS rDNA and LSU rDNA

About 50 swimming cells from each *P. cunningtonii* culture were submitted to DNA extraction with the QuickExtract™ FFPE DNA Extraction Kit (epicentre, Illumina, San Diego, California, USA), following the manufacturer's instructions. Two microlitres of extracted DNA were used in all PCR amplifications conducted. Amplification of LSU rDNA of *P. cunningtonii* strain 2 was as described above for strain 1 with the single modification of using the specific Dino-ND primer (Hansen and Daugbjerg 2004) instead of the 28-1483R primer, in both initial and nested PCRs. Amplifications of SSU rDNA and ITS rDNA of *P. cunningtonii* strain 1 were based on Takano and Horiguchi (2005) but going directly to the second round of PCR amplification. The products from all PCR amplifications were purified with the QIAquick PCR Purification Kit (Qiagen, Hilden, Germany), and sent to Macrogen Europe (Amsterdam, The Netherlands) for sequencing of SSU rDNA and ITS rDNA from *P. cunningtonii* strain 1, with

primers as in Takano and Horiguchi (2005), and for sequencing of LSU rDNA from *P. cunningtonii* strain 2 using D1R, D2C, D3A, D3B and Dino-ND (Hansen and Daugbjerg 2004; Nunn et al. 1996; Scholin et al 1994).

Sequence divergence

PAUP* (ver. 4.0a, build 169) was used to estimate the divergence between the partial sequences of the nuclear-encoded LSU rDNA of the two strains (Swofford 2002).

Phylogeny

Two sequence data matrices were prepared to infer the phylogeny of the two isolates of *P. cunningtonii*. The first comprised partial sequences of nuclear-encoded LSU rDNA (1,635 base pairs including introduced gaps) from *P. cunningtonii* strain 2 and *P. cunningtonii* strain 1 together with a diverse assemblage of dinoflagellates (52 genera, 84 different taxa). Ciliates, apicomplexans and *Perkinsus* formed the outgroup taxa. For the second analysis based on concatenation of the ribosomal operon (3,923 base pairs including introduced gaps of partial SSU rDNA, ITS 1, 5.8S rDNA, ITS 2 and partial LSU rDNA) only strain 1 was included together with some of the most closely related lineages inferred from the LSU rDNA-based phylogeny. However, due to lack of sequence data for some rDNA fragments, '*Peridinium inconspicuum*' and '*Peridinium centenniale*' were replaced with *Parvodinium trawinskii* Kretschmann, Owsiany, Zerdoner & Gottschling and *P. marciniaakii* Kretschmann, Owsiany, Zerdoner & Gottschling. Therefore, the LSU rDNA phylogeny comprised a total of 12 *Parvodinium* sequences whereas the concatenated phylogeny included 10 *Parvodinium* sequences. Other included dinoflagellates belonged to e.g., *Palatinus*, *Peridinium* Ehrenberg, *Johsia* and *Scrippsiella* Balech. Two species of *Heterocapsa* F. Stein formed the outgroup. See Pandeirada et al. (2022) for information on alignments and sequence editing. Two approaches were applied for phylogenetic inference: Bayesian analysis (BA) and RAxML as implemented in Geneious (ver. 2022.1.1). Common for both BA (ver. 3.2.6 of MrBayes by Huelsenbeck and Ronquist (2001)) 5 million generations were run with a tree sampled every 1,000 generations. The burn-in length was set at 500,000 leaving 4,501 trees for the consensus tree. Specifically for the concatenated data matrix, each genetic marker was divided into five partitions (SSU, ITS1, 5.8S, ITS2 and LSU) and allowed to evolve under different models of sequence evolution by applying the 'un-link' option in the command script. For RAxML (ver. 8, Stamatakis 2014) the GTR GAMMA I option was used with both alignments and 1,000 bootstrap replications were included to evaluate the robustness of the tree topologies. These values were mapped onto BA trees.

Results

The external morphology of strain 2 agrees with the morphology of typical *Peridiniopsis cunningtonii*. In contrast, strain 1 shows a slight difference in LSU rDNA sequence and a constant, apparently inheritable, difference in morphology from strain 2, which we consider worthy of formal recognition at variety level within *P. cunningtonii*. In our phylogenetic analyses both strains resolved in the same clade as *Parvodinium* species, justifying a new combination in *Parvodinium*. To avoid confusion in referring to the two strains in the following text we will use the names formally established later in the article: *Parvodinium cunningtonii* var. *cunningtonii* for strain 2, and *P. cunningtonii* var. *inermis* var. nov. for strain 1 (see Taxonomic summary).

The cultures of both strains were unialgal and presumably monoclonal since they both resulted from single cells. These cultures diverged markedly in asexual growth. Gamete fusion was not detected in either strain, despite the observation of cysts in cultures of *Parvodinium cunningtonii* var. *inermis* var. nov. Cyst formation and germination were not followed, and an archeopyle was not observed. *Parvodinium cunningtonii* var. *inermis* has been in culture for about seven years and has usually high numbers of motile cells. *Parvodinium cunningtonii* var. *cunningtonii* persisted in culture only for about half a year, always with very low numbers of motile cells and without the formation of cysts.

Cell morphology of *Parvodinium cunningtonii* var. *inermis* var. nov.

Motile cells and cysts are shown in Figs. 1 and 2. Cells were ovoid to pyriform and somewhat compressed dorsoventrally (Figs. 1A–D; 2A–C). The epicone was conical, with an apical pore complex (apc) in the prominent apex, and was longer than the round to conical, antapically pointed hypocone (Figs. 1A–D; 2A–F). The submedian cingulum was almost circular (Figs. 1A–D; 2A–C; 2F). The sulcus somewhat penetrated the epicone, and extended also toward the antapex (Fig. 2A, B, F). Cells were 24.1 ± 2.9 μm long (range 17.7–30.0 μm ; $n = 60$), 17.1 ± 2.4 μm wide (range 11.8–20.7 μm ; $n = 41$), and 14.4 ± 0.9 μm thick (range 12.7–16.4 μm ; $n = 14$).

Chloroplast lobes were yellowish-brown and radiated from a central pyrenoid to the cell periphery (Fig. 1A–D). One accumulation body (ac) was sometimes notorious above the central pyrenoid (Fig. 1B). The nucleus was ellipsoid and occupied most of the hypocone (Fig. 1B, D). A rectangular, orange eyespot, somewhat slanted relative to the longitudinal axis of the cell, 3.0–4.5 μm long ($n = 12$), was present in the upper part of the sulcus (Fig. 1A, C).

The plate tabulation was po, cp, x, 4', 1a, 6'', 6c, 5 s, 5''', 2'''' (Kofoidian notation). The epitheca included four apical

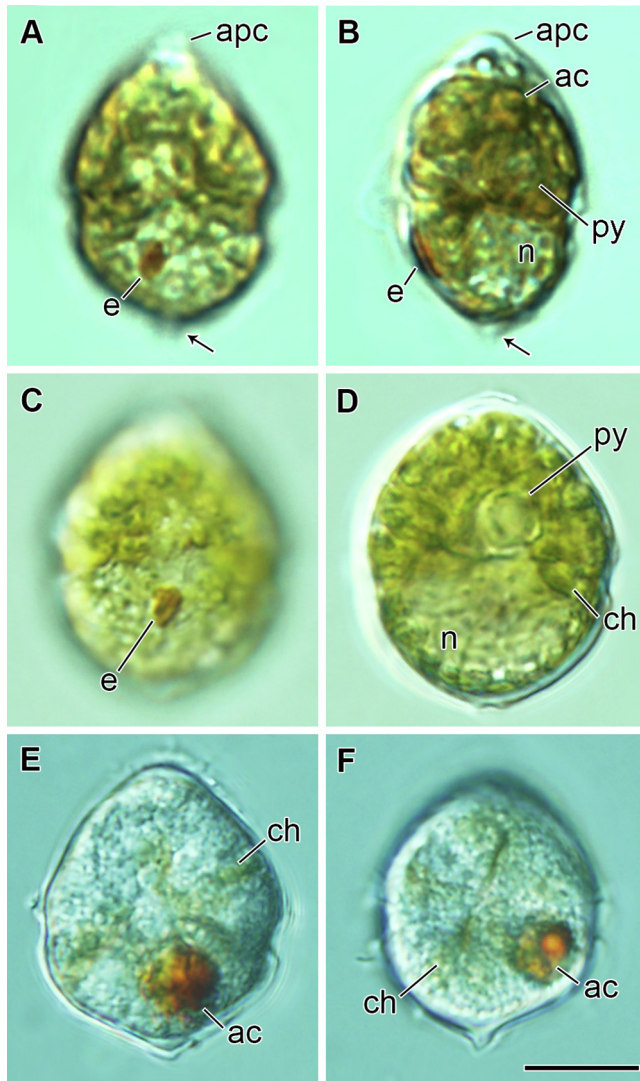


Fig. 1. *Parvodium cunningtonii* var. *inerme* var. nov., LM. (A, B) Ventral and left-lateral views of vegetative cell showing the pointed antapical end (arrow), the apical pore complex (apc), the eyespot (e), the nucleus (n) in the hypocone, and the pyrenoid (py) and accumulation body (ac) in the epicone. (C, D) Vegetative cell focused in different planes showing the eyespot (e), the nucleus (n) and chloroplast lobes (ch) radiating from the central pyrenoid (py). (E, F) Cysts smooth-walled, with similar shape as the vegetative cells. Cyst contents are predominantly colourless with faint traces of chloroplast lobes (ch) and a large accumulation body (ac). All to the same scale. Scale bar: 10 μ m.

plates, six precingular plates, and a single anterior intercalary plate 1a on the left-dorsal side (Fig. 2A–D). Some variation of the epithecal tabulation was observed; out of 27 cells analysed, 21 had the usual plate tabulation (4', 1a), two cells had four apical and zero anterior intercalary plates (4', 0a; not shown) and four cells had five apical and zero anterior intercalary plates (5', 0a; Fig. 2E). Three plates formed the apc: a central cover plate (cp) encircled by the pore plate (po), and a rectangular canal plate (x)

tightly appressed to the ventral side of po (Fig. 2D, E). On the hypotheca there were two antapical plates (1''' and 2''') of similar size, and five postcingular plates, of which 3''' was the largest and 5''' the smallest (Fig. 2A–C, F). The sulcus was composed of five plates: an anterior sulcal plate (as) extending somewhat into the epitheca; a larger, posterior sulcal plate (ps) extending to the antapex; a right sulcal (rs) plate extending as a flap, hiding the exit pores of the flagella and peduncle, and partially overlapping the left (ls) and the small accessory sulcal plates (acs) (Fig. 2A, B, F). Six plates formed the cingulum, of which the first plate (c1) was shorter and partially included in the anterior-left side of the sulcus (Fig. 2A–C, F). The sixth cingular plate (c6) descended slightly distally by nearly half the cingulum width (Fig. 2A, B). The limits of this plate (c6) coincided roughly with the limits of the sixth precingular (6'') and fifth postcingular (5''') plates; similarly, the limits of plates c4 and c5 were coincident with those of postcingular plates 3''' and 4''', respectively (Fig. 2A–C, F). An antapical projection (apiculus), 0.5–1.8 μ m long (n = 15), typically occurred in plate 1''', near the suture with plate 2''', or right at the suture between antapical plates (Fig. 2B, C, F).

Plates were smooth and the observed sutures were thin. Trichocyst pores occurred throughout the cell surface but were absent from the apc and from the right and left sulcal plates (Fig. 2B–F). Cells that stopped swimming exited the theca through the dorsal side, with at least the fourth precingular plate being discarded (not shown).

Cyst walls were smooth, apparently including an endospore, and matched the shape of the motile cells (a pointed cyst with submedian paracingulum); they were almost colourless with faint traces of chloroplast lobes and contained an orange-red accumulation body (Fig. 1E, F). Cysts were 20.5–28.0 μ m long and 13.5–24.0 μ m wide (n = 27).

Cell division in *Parvodium cunningtonii* var. *inerme* var. nov.

Division stages were observed in immobile cells that were isolated from the bottom of the culture batches into separate wells with culture medium and followed using the inverted microscope. These immobile cells were morphologically similar to motile cells, except for the absence of flagella (Fig. 3A), and were more abundant during the first two or three hours of the light phase. The nucleus of these cells migrated from the hypocone to the epicone over a period of 1–3 h (Fig. 3A, B), followed by nuclear division that progressed for about 4 h (Fig. 3C, D). Cytokinesis started shortly after the two separated nuclei were clearly visible in the cell, with a cleavage furrow progressively extending to the area between the nuclei (Fig. 3D, E). About 1.5 h since the cleavage furrow started to become visible, the incompletely divided daughter cells emerged, with a gentle amoeboid movement, through the dorsal side of the

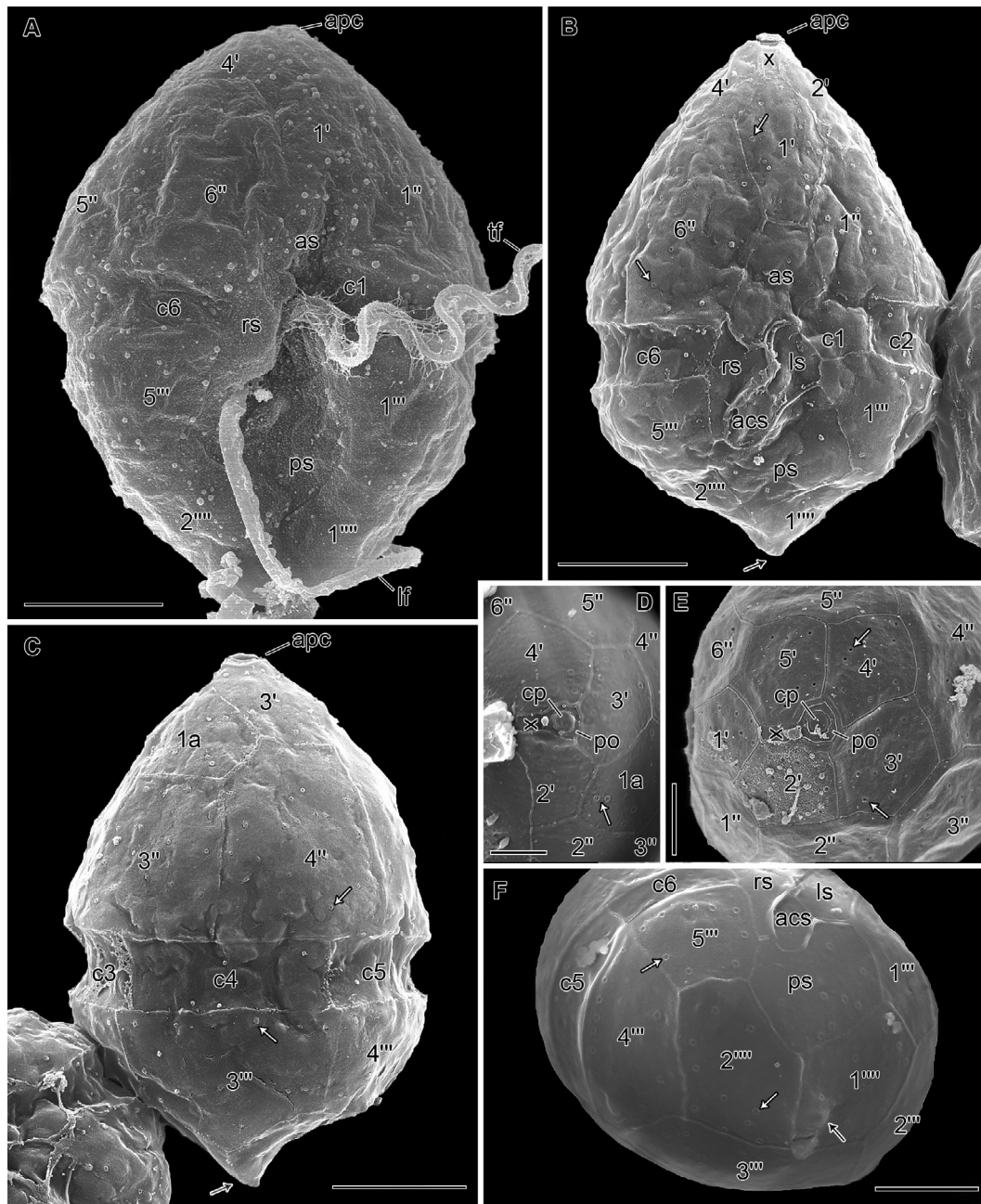


Fig. 2. *Parvodinium cunningtonii* var. *inerme* var. nov., SEM. Plates are labelled in Kofoidian notation. (A) Ventral view of a cell with preserved outer membranes and transverse (tf) and longitudinal flagella (lf), prepared with fixation 3. (B–C) Ventral and dorsal/right view of cells prepared with fixation protocol 2. Five plates form the sulcus: anterior (as), right (rs), left (ls) and posterior (ps) sulcal plates, plus smaller accessory sulcal plate (acs) (seen in A, B, F). (D–E) Apical views of cells prepared with fixation 1, showing the typical tabulation with one intercalary plate (in D) and one variation with five apical plates and no intercalary plate (in E). Apical pore complex (apc) with pore plate (po), cover plate (cp) and canal plate (x). (F) Antapical view of a cell prepared with fixation 2. The pointed antapical end is indicated by a black arrow and trichocysts pores by white arrows. Scale bars: 5 μm (A–C, F); 3 μm (D, E).

theca, at the level of the cingulum (Fig. 3F–H). The released, incompletely divided cells showed two separate hypocones, each one with a nucleus and an eyespot (e), and only one epicone and one cingulum (Fig. 3F, H). Two longitudinal flagella and one or two transverse flagella were usually present, but they were not in the furrows at this

stage. The dividing cell remained motionless for a few seconds and sunk; it started to swim after the flagella were accommodated in the cingulum and both sulci (Fig. 3G, H). This swimming stage continued for about 6 h, up to the first 3–4 h of the dark phase. The division and final separation of the two cells was never observed, showing that

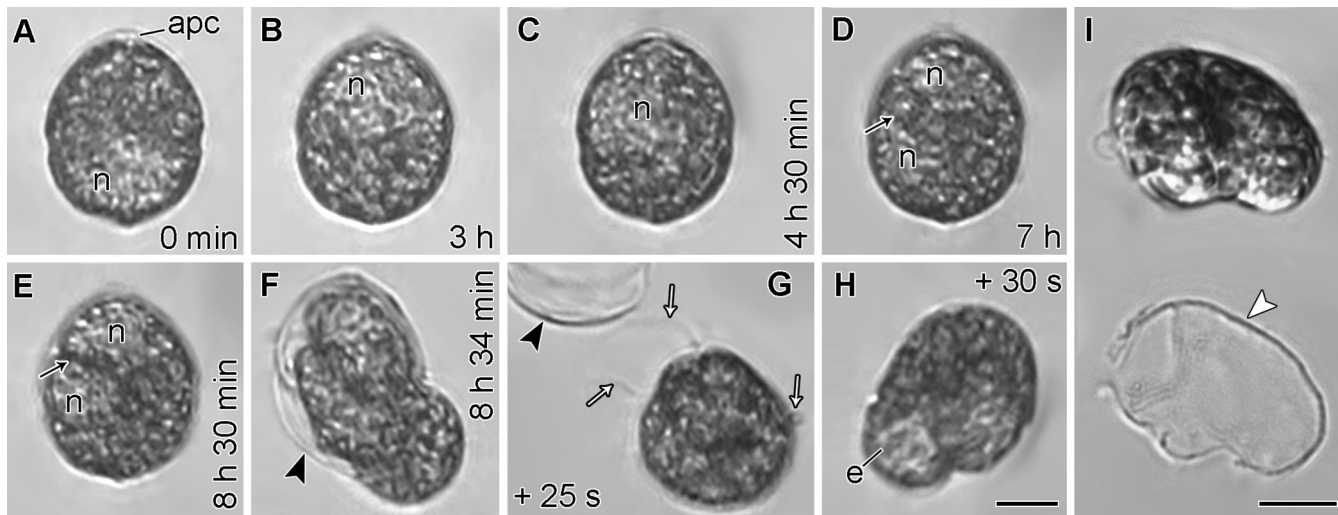


Fig. 3. *Parvodinium cunningtonii* var. *inerme* var. nov., LM. (A–H) Division of an immobile cell. Image-series from video recording, with elapsed time indicated. (A) Cell without flagella with the nucleus (n) in the hypocone. apc, apical pore complex. (B–E) Nuclear migration to the epicone, where mitosis took place. A cleavage furrow is seen (D, E) between the two nuclei formed. (F–H) Incompletely divided daughter cells exited the theca (arrowhead). Arrows point two longitudinal flagella and transverse flagellum in G. The eyespot in one hypocone is visible (e, in H). (I) Another cell in division that stopped swimming and exited the theca (arrowhead). Scale bars: 10 μ m.

the complete process of division was very long (more than 15 h). Similar swimming stages were observed in the culture throughout the light and dark phases, with more or less developed thecal plates that were shed during temporary stops (Fig. 3I). No evidence of fusion of cells, or planozygotes (flagellated cells with two sulcal flagella) was ever observed in this culture. The cysts observed were therefore perhaps of asexual origin. However, based on the presence of a thick wall they may be interpreted as resting cysts.

Cell morphology of *Parvodinium cunningtonii* var. *cunningtonii*

Motile cells and empty thecae, with plates marked in Kofoidian notation, are shown in Fig. 4. Cells were ovoid and somewhat compressed dorsoventrally (Fig. 4A–J, L, M). The epicone was conical, topped with an apical pore complex (apc) and slightly longer than the rounded-trapezoidal hypocone, which presented antapical and postcingular spines (Fig. 4). The cingulum was almost circular (Fig. 4C–E, M). The sulcus penetrated the epicone and extended toward the antapex (Fig. 4E, H, M). Cells were 26–32 μ m long ($n = 12$) and 19–25 μ m wide ($n = 10$).

Chloroplast lobes were yellowish-brown and radiated from the centre of the cell to the periphery; a pyrenoid was not clearly visible in LM. One accumulation body (ac) was usually prominent in the epicone (Fig. 4A–D). In the upper part of the sulcus was a rectangular dark-orange eyespot (e) somewhat slanted relative to the cell axis, 3.5–4.0 μ m long ($n = 5$) (Fig. 4A–D). The nucleus (n) was ellipsoid and occupied part of the hypocone (Fig. 4D).

The plate tabulation was po, cp, x, 4', 1a, 6'', 6c, 5 s, 5''', 2'''. No variations were detected in the number of intercalary and apical plates in the cells observed. The apical plates were all six-sided, while the precingular plates and the anterior intercalary plate were five-sided; the postcingular plates were all four-sided and somewhat trapezoid except for plate 3''', which was five-sided; the antapical plates were both five-sided. All plates were lightly reticulated, and sometimes separated by wide sutures; the hypothecal plates were ornamented with spines. In most cells all postcingular and antapical plates, except plate 3''', had at least one spine, and cells with two spines in some plates (most commonly plates 1'', 5'', 1'''' and 2''') were sometimes observed (Fig. 4E–J, L, M). The longest spines were in the antapical plates (1'''' and 2''') and were up to 5 μ m long.

General fine structure (TEM)

The general fine structure observed in cells of the two strains was similar (Fig. 5). The ellipsoid nucleus was in the mid-dorsal side of the hypocone (Fig. 5A). Chloroplast lobes (ch), with thylakoids in groups of three per lamella, radiated in all directions from a prominent pyrenoid (py) located in the epicone; at the periphery of the cell, the chloroplast lobes extended tangentially, covering most of the cell surface (Fig. 5A, D, E). The pyrenoid was surrounded by starch (st) and its matrix was perforated by numerous, scattered cytoplasmic channels, mostly ca. 40 nm in diameter; pusular elements were also observed in a few, wider cytoplasmic channels (Fig. 5E, F). Tri-

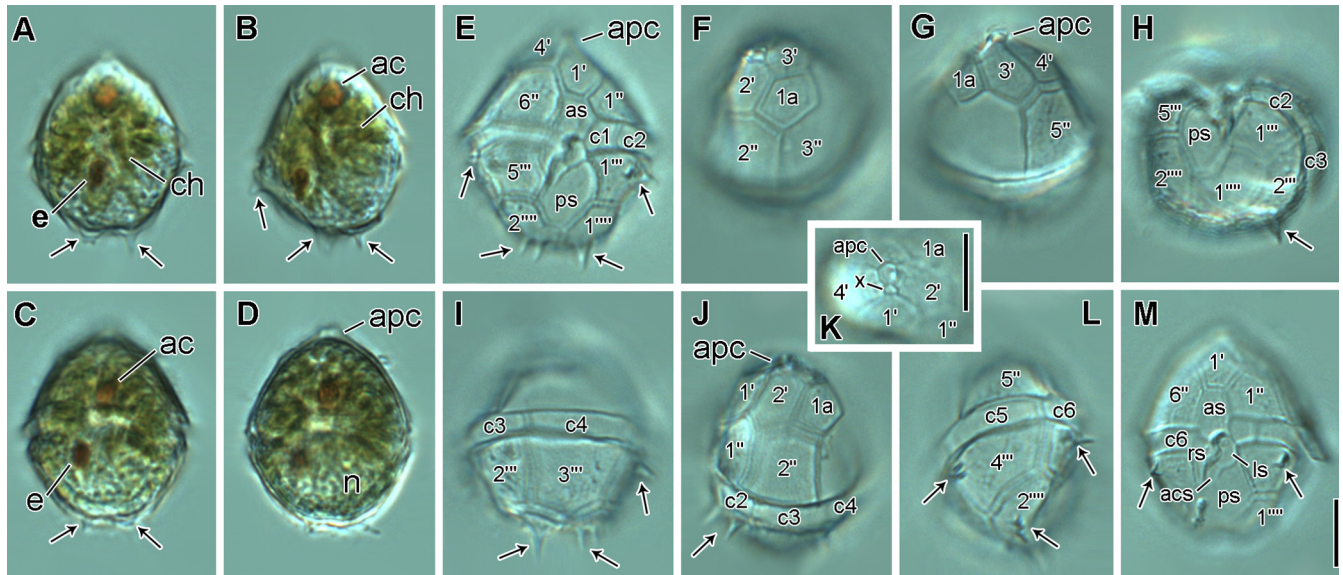


Fig. 4. *Parvodinium cunningtonii* var. *cunningtonii*, LM. (A, B) Ventral and left-ventral views of one cell with chloroplast lobes (ch) radiating from the centre, an accumulation body (ac) in the epicone and the eyespot in the sulcal region. Antapical and postcingular spines are prominent (arrows). apc, apical pore complex. (C, D) Ventral view and optical section of a cell with short spines in the hypotheca, the nucleus (n) in the hypocone, the eyespot (e) and accumulation body (ac); the apical pore complex (apc) is indicated. (E–L) Empty theca in different views showing plates labelled in Kofoidian notation. Antapical and postcingular plates with prominent spines (arrows). The apical pore complex (apc) includes a short canal plate (x). (M) Ventral view of a different theca with two postcingular spines (arrows) visible. The five sulcal plates are indicated: anterior (as), right (rs), left (ls), posterior (ps) and the smaller accessory sulcal plate (acs). Scale bars: 10 µm; (A–J, L, M) to the same scale.

chocysts (t) were usually present in the peripheral cytoplasm (Fig. 5A, C, E). Starch grains were scattered in the cell but were more numerous in the hypocone, whereas oil droplets (o) were more abundant in the epicone (Fig. 5A). An eyespot, consisting of four to five layers of globules inside the ventral surface of a chloroplast lobe, was present in the sulcus (Fig. 5A, B). In distal portions of this chloroplast lobe, near the edge of the eyespot, the layers of globules were shorter and partially intercalated with thylakoid bands (not shown). Each individual globule measured 100 to 120 nm in diameter.

Longitudinal sections through the apical pore complex (apc) exposed an apparently continuous fibrous layer (Fig. 6A–D) underlying the pore plate (po). The posterior portion of the fibrous layer subdivided into several somewhat striated fibers that extended along the peripheral cytoplasm for about 500 nm (arrowheads in Fig. 6E). The cytoplasm of this apical region was rich in irregularly shaped vesicles with clear contents and elongated necks that extended toward the cover plate (white arrows in Fig. 6A–C).

Pusular system

In both *Parvodinium cunningtonii* strains, two sets of pusular elements (membrane-bounded compartments wrapped in a vesicle) were observed, each one associated with one of the flagellar canals (Figs. 7; 8E; 9B, C; 10A,

B, H; 11E; 12A). One pusular tube (pu), more or less flattened in some regions, opened at the transverse flagellar canal (TFC) and extended to the dorsal-right side of the cell with several ramifications (Figs. 7A, C–E; 10A, B). At least one of these ramified pusular tubes extended into the pyrenoid and was visible inside cytoplasmic channels that penetrated chloroplast lobes and the pyrenoid (Figs. 5E, F; 7A, F). This pusular tube, near the connection to the TFC, was ca. 300 nm wide and had the three pusular membranes usually closely appressed (Figs. 9B, C; 10A, B). In other portions, along the extension of the ramified pusular tube, the surrounding vesicle had numerous fenestrations, resulting from links between its outer and inner membranes, which left the inner membrane of the pusule in contact with the cytoplasm (arrows, Fig. 7B). Some portions of the pusular tube were internally lined by electron-opaque granules ca. 15 nm in diameter (Figs. 5F; 7E, F). Connected to the longitudinal flagellar canal (LFC), there was a pusular vesicle (puv), slightly collapsed and with an irregular shape, that ramified and extended c. 3.5 µm toward the centre of the cell (Figs. 7G; 8E; 10H). The lumen of this puv included several vesicles with irregularly shaped granulated bodies (arrowheads in Figs. 7G; 8E; 10H).

Flagellar apparatus

The flagellar apparatus of the two strains was identical and is here shown in series of sections from a cell of *Par-*

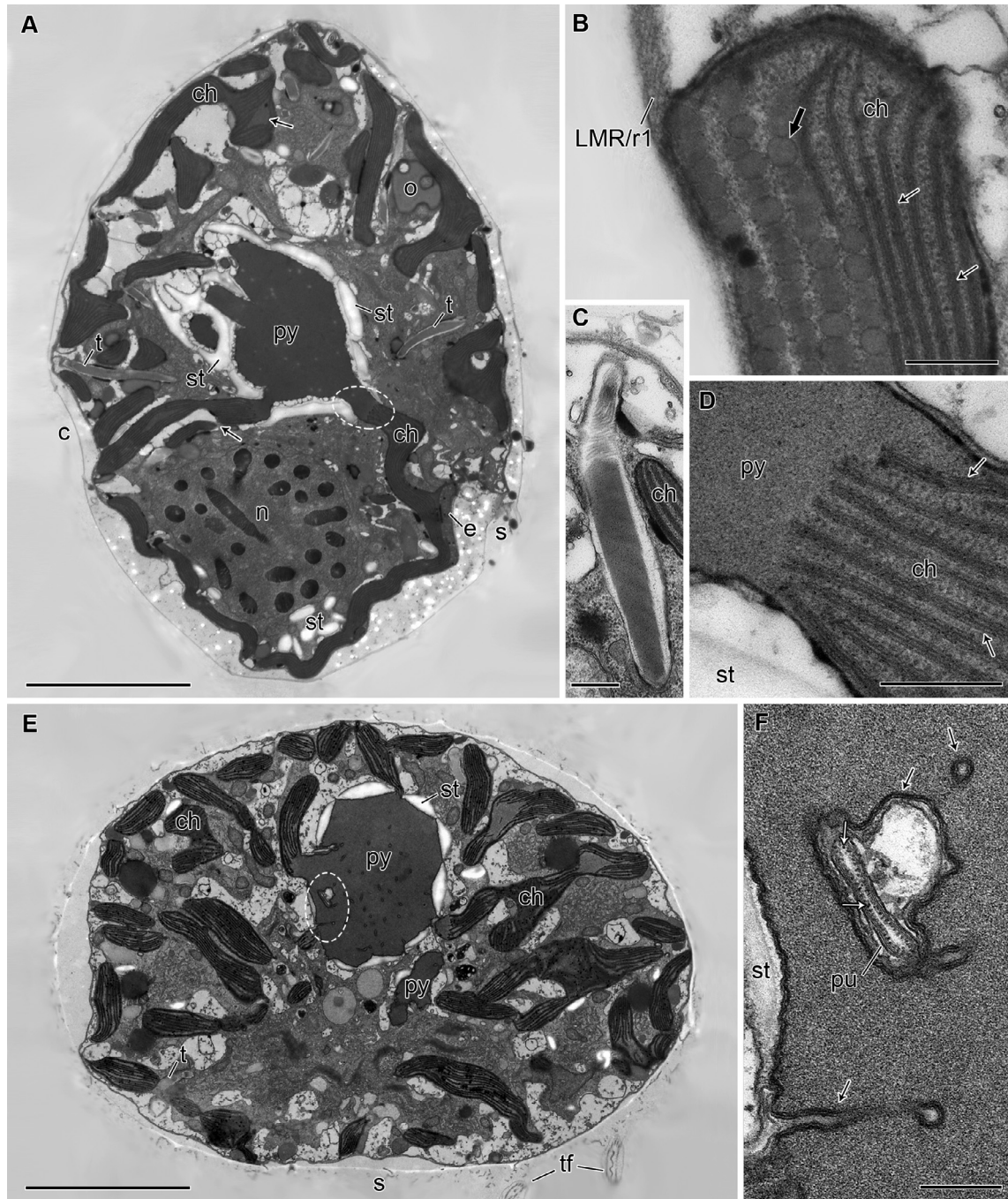


Fig. 5. *Parvodinium cunningtonii* var. *inerme* var. nov. (A–D) and *P. cunningtonii* var. *cunningtonii* (E, F), general ultrastructural features, TEM. (A) Longitudinal section of a cell view from the right side, showing the position of the nucleus (n) and chloroplast lobes (ch) radiating from the central pyrenoid (py). Ramifications and thylakoid-free areas visible in radiating lobes (arrows). e, eyespot; t, trichocysts; o, oil droplets; st, starch; c, cingulum; s, sulcus. (B) Detail of eyespot with four adjacent rows of globules (thick arrow) disposed along the ventral surface of a chloroplast lobe, in front of the thylakoids (thin arrows). The longitudinal microtubular root (LMR/r1) lays between the cell surface and the chloroplast lobe. (C) Longitudinal section of a trichocyst. (D) Chloroplast lobe (ch) radiating from the central pyrenoid (py) complex (ellipse in A), showing the three-thylakoid lamella (arrows). (E) Transverse section in apical view of a cell sectioned above the cingulum level showing the chloroplast lobes (ch) radiating from the pyrenoid (py) surrounded by starch (st). s, sulcal area; tf, transverse flagella. (F) Magnification of pyrenoid matrix (ellipse in E) traversed by cytoplasmic channels (black arrows); the larger cytoplasmic channel includes a pusular element (pu) with dotted lumen (white arrows). Scale bars: 5 μ m (A, E); 300 nm (B–D, F).

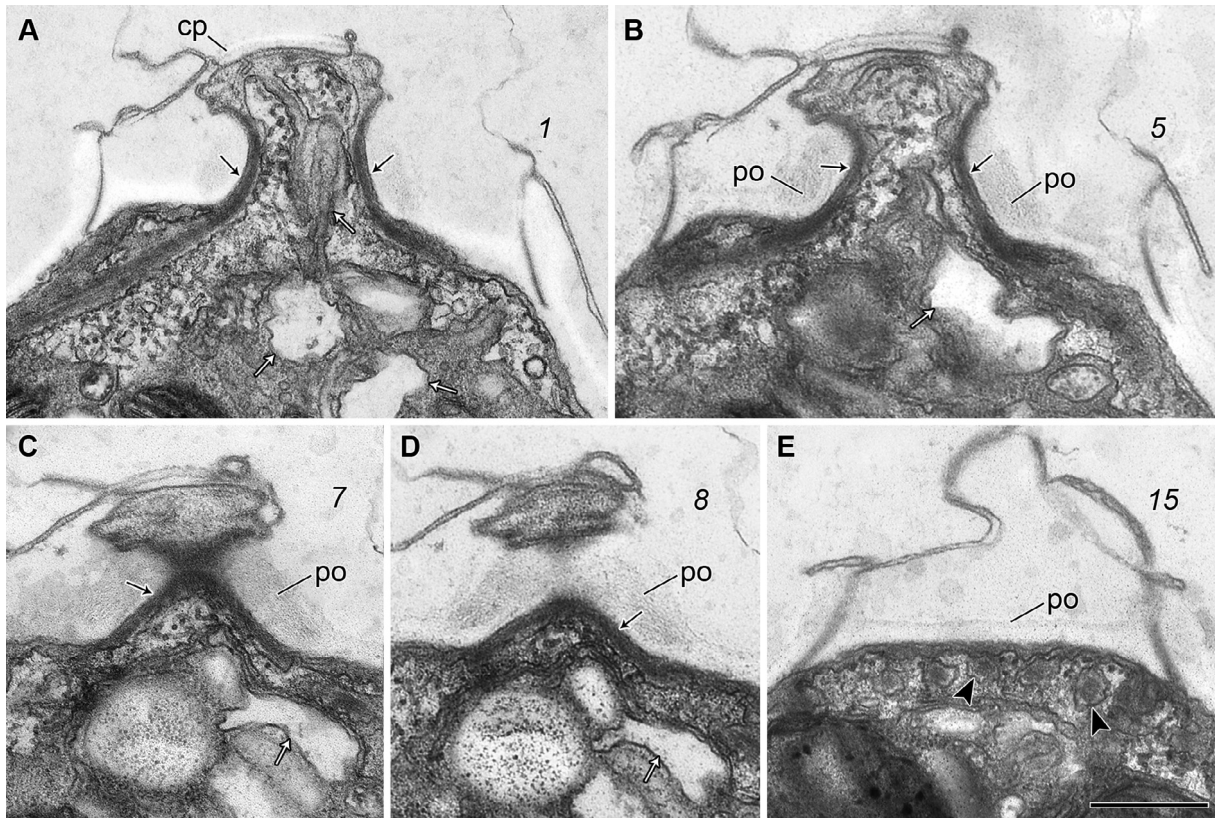


Fig. 6. *Parvodinium cunningtonii* var. *cunningtonii*, apical pore complex, TEM (initial fixative containing OsO₄). Non-adjacent oblique-longitudinal serial sections, proceeding from the anterior-right side of the cell. Slanted numbers represent section numbers. (A, B) Sections through the pore plate (po) with enclosed cytoplasm, and the cover plate (cp). Fibrous layer is marked (black arrows) underneath the po and extending to the apical-most cytoplasm. Several vesicles extend towards the cp (white arrows). (C, D) Tangential sections through the pore plate (po) and the cover plate (cp), showing fibres (black arrows) and vesicles (white arrows). (E) Individualized fibres (arrowheads) in cross section underneath the Po. Scale bar: 500 nm.

vodinium cunningtonii var. *inerme*, advancing from the apex to the antapex of the cell (Fig. 8A–H) and from two cells of *P. cunningtonii* var. *cunningtonii*, one also sectioned from the apex to the antapex but slightly tilted to the right (Fig. 10A–H) and a second one sectioned from right to left (Fig. 11A–E). The two basal bodies formed an angle of about 90°, as inferred from serial sections, and had their proximal ends almost touching (Fig. 8E). The points of emergence of the transverse and longitudinal flagella (TF and LF, respectively) were surrounded by rings of striated material (the TSC and LSC, transverse and longitudinal striated collar, respectively). The transverse basal body (TB) was associated with two microtubular roots. A single microtubule, the transverse microtubular root (TMR/r3), curved along the anterior-ventral side of the transverse flagellar canal (TFC), near a small row of collared pits (arrowheads in Fig. 8B, C), and associated with the anterior-dorsal base of the TB (Figs. 8B–D; 10B; 11B). In its distal end, the TMR nucleated a strand of ca. 22 microtubules, the so-called transverse microtubular root extension (TMRE/r3E), which followed the anterior side of the TFC and then curved along its dorsal side into a poste-

rior direction for about 1.5 μm, until it suddenly turned to the dorsal side of the cell (Figs. 9A–C; 11C–E; 12A). The second microtubular root associated with the TB was a single microtubule running alongside a striated fibre (TSR and TSRM/r4); the TSR was ca. 40 nm thick and together with the TSRM/r4 extended from the proximal-dorsal side of the TB for about 400 nm toward the TSC (Figs. 8G, H; 9A; 10B, C). The longitudinal basal body (LB) was also linked to two microtubular roots: a single-stranded microtubular root (SMR/r2) that started near the proximal-right side of the LB and curved slightly into a dorsal-posterior direction for about 550 nm; the second microtubular root was a strand of ca. seven microtubules (the longitudinal microtubular root, LMR/r1) that associated with the proximal-left side of the LB and curved slightly into a dorsal-posterior direction, in a roughly parallel route to the SMR/r2; the number of microtubules increased posteriorly to about 30, which came to lie underneath the cell surface down to the level of the eyespot (Figs. 5B; 7D, G; 8F–H; 9A–C; 10E–H; 11B). The two basal bodies were indirectly linked by a layered structure, the so-called layered connective (LC), which in transverse section was ca. 74 nm thick, 105 nm wide and

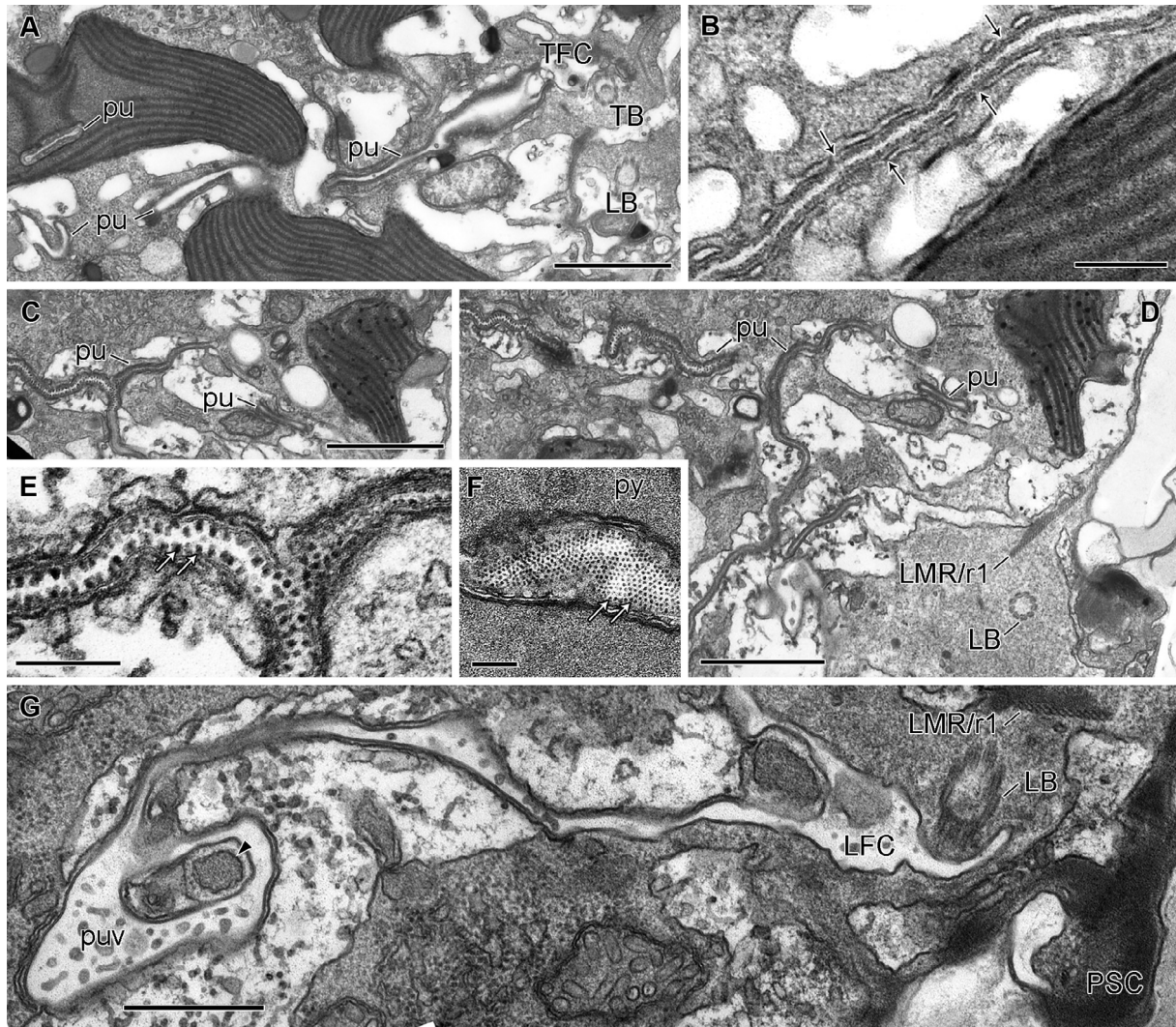


Fig. 7. *Parvodinium cunningtonii* var. *inerme* var. nov. (A, B) and *P. cunningtonii* var. *cunningtonii* (C–F), pusular system, TEM. (A) Pusular tube (pu) connecting to the transverse flagellar canal (TFC) and extending from the ventral area to the centre of the cell. A portion of the pusular tube is seen included in a chloroplast lobe. TB, transverse basal body. (B) Detail of pusular tube with the enveloping vesicle, showing fenestrations (black arrows). (C, D) Pusular flattened tubes (pu) ramify and extend from the ventral region to the interior of the cell. (E) Detail of ramified portion of the pusular tube with dotted contents (arrows). (F) Tangential section through a pusular tube with dotted content (arrows) that penetrates the pyrenoid (py). (G) Pusular vesicle (puv) with vesicle including a granulated body (arrowhead), associated to the longitudinal flagellar canal (LFC). LB, longitudinal basal body; LMR/r1, longitudinal microtubular root; PSC, peduncle striated collar. Scale bars: 1 μ m (A, C, D); 200 nm (B, E, F); 500 nm (G).

280 nm long. The LC was made of two electron-opaque layers separated by a more electron-translucent layer, and contacted with its anterior surface the TB, and with the posterior surface an electron-opaque layer of material that covered the dorsal side of the LMR/r1 (Figs. 8G–H; 11B). The proximal end of the TSR and TSRM/r4 also contacted the anterior layer of the LC. Two or three small fibres linked the dorsal face of the proximal end of the LMR to two or three triplets of the posterior side of the TB (Fig. 11B).

Peduncle and microtubular strand of the peduncle (MSP)

An extruded peduncle was observed in sections of both *Parvodinium cunningtonii* var. *cunningtonii* and *P. cunningtonii* var. *inerme* (Figs. 9A; 10G; 11D). The peduncle was composed of cytoplasm lined by a single-membrane, and included a group of ca. 20 microtubules, the so-called microtubular strand of the peduncle (MSP). The peduncle

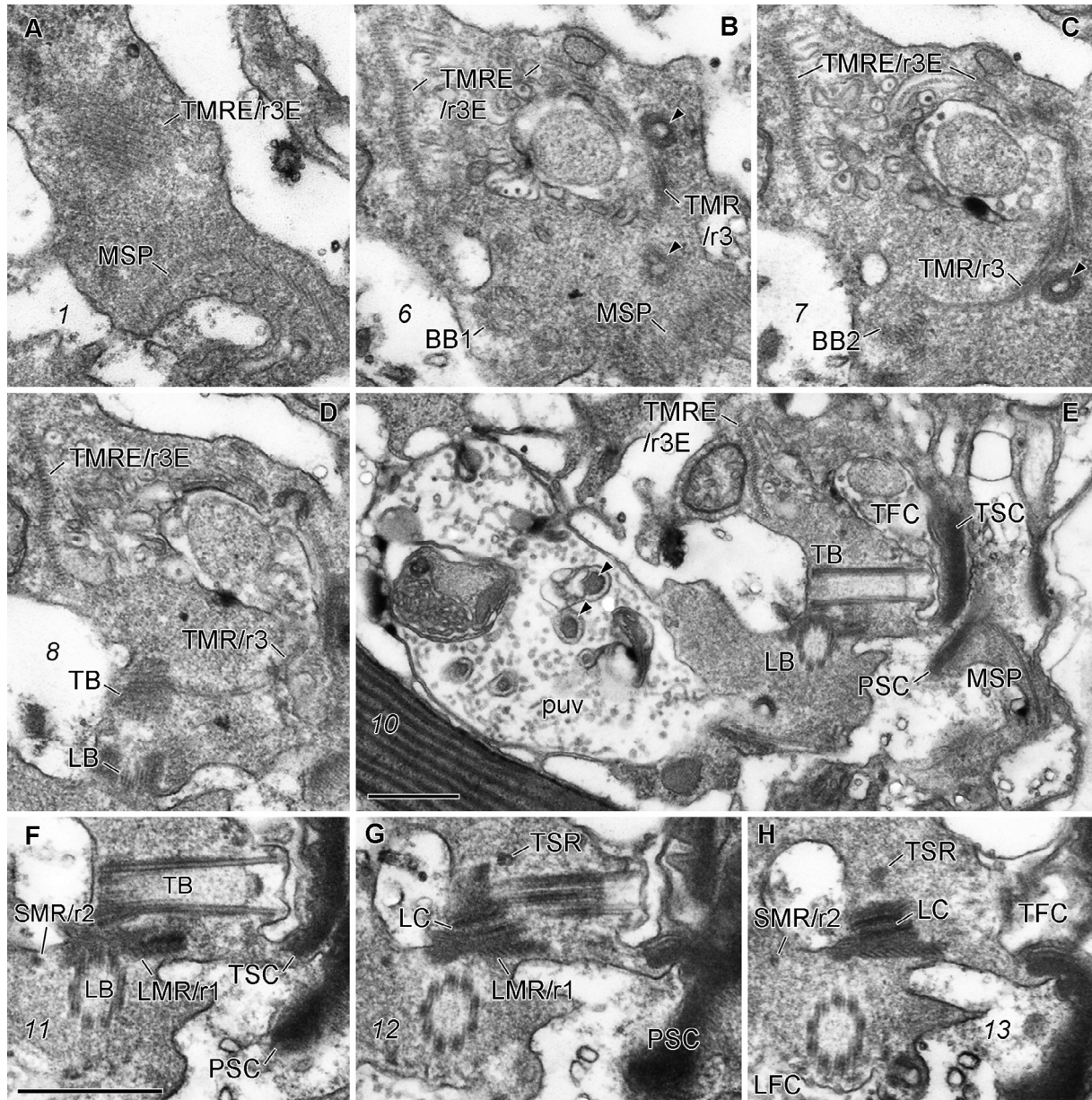
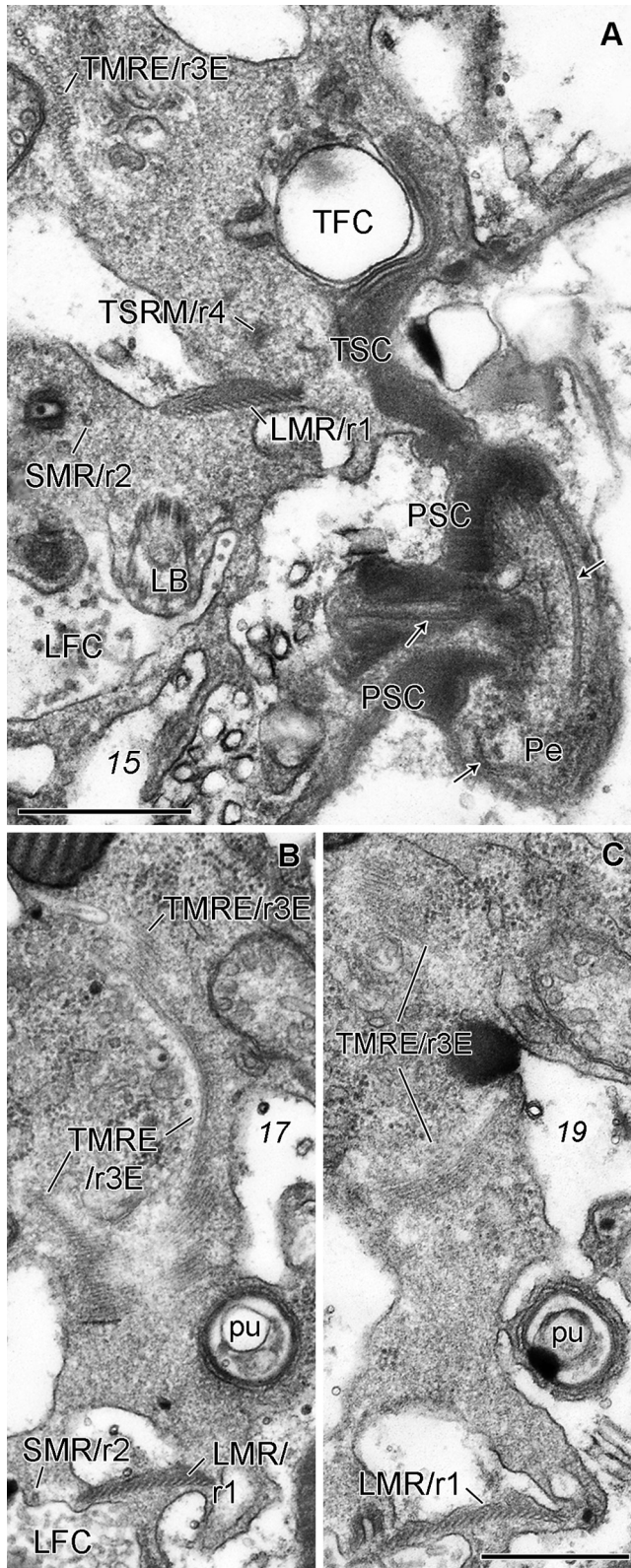


Fig. 8. *Parvodinium cunningtonii* var. *inerme* var. nov., flagellar apparatus, TEM. Non-adjacent serial sections progressing from the apex to the antapex of a cell slightly tilted to the dorsal side. Slanted numbers indicate the section number. (A–D) The microtubular strand of the peduncle (MSP) and the transverse microtubular root extension (TMRE/r3E) are seen progressing to the basal bodies. The transverse microtubular root (TMR/r3) that nucleates the TMRE/r3E is seen near collared pits (arrowheads), ending near the transverse basal body (TB). Two replicated basal bodies (BB1, BB2) are visible in B and C. (E) Both basal bodies, the TB and the longitudinal basal body (LB), and the MSP are visible as well as the transverse striated collar (TSC) and the peduncle striated collar (PSC). A large pusular vesicle (puv) is seen to emerge from the longitudinal flagellar canal and includes vesicles with granulated bodies (arrowheads). (F–H) The single-stranded microtubular root (SMR/r2) and the longitudinal microtubular root (LMR/r1) are present on the left and right side of the LB, respectively. The layered connective (LC) appears between the LB and TB. TSR, transverse striated root. Scale bars: 500 nm; (A–D, F–H) to the same scale.

extruded through a collar of fibrous material, the so-called peduncular striated collar (PSC) and extended to the exterior of the cell through a narrow canal, ca. 1.3 μm long \times 0.4 μm high \times 0.25 μm wide. It was lined by 4–6 platelets with a somewhat fibrous aspect, different from that

of the larger plates (Fig. 10G, H). Outside the cell, the peduncle was up to 3.5 μm long and 1.5 μm wide. The MSP extended to the interior of the cell, arranged as two slightly overlapping rows of about 20 and 15 microtubules each, accompanied in this ventral area of the cell by several



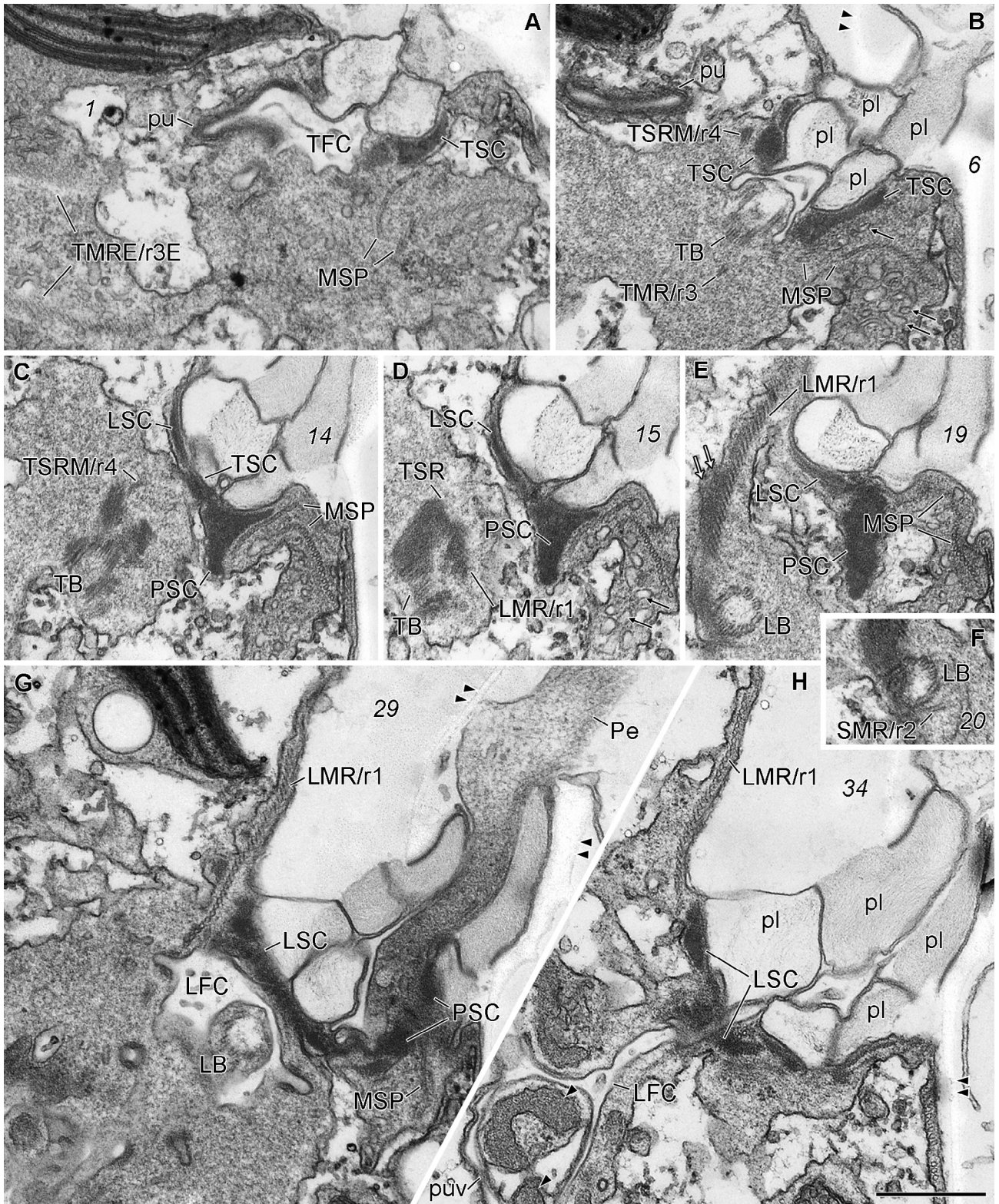
tubular vesicles with clear contents (arrows in Fig. 10B, D). Electron-opaque bodies were not detected along the MSP. The MSP had an estimated path in the cell of 15–20 μm , ascending on the ventral right side of the basal bodies, slightly curving to the ventral-left side of the central pyrenoid and up to near an accumulation body (Figs. 10A–G; 11A, B; 12B). Here it curved and extended back to the right side of the cell, passing on the ventral side of the pyrenoid (Fig. 12A, B). It ended between the pyrenoid and the nucleus, almost reaching the distal end of the TMRE/r3E (not shown).

Sequence divergence and phylogeny

The genetic distance (sequence divergence) between the two strains of *P. cunningtonii* was calculated based on the Kimura-2-parameter model and it had a value of 0.0032. This estimate was based on four substitutions out of 1,260 base pairs of the nuclear-encoded LSU rDNA being compared.

The tree topology based on partial LSU rDNA included a diverse assemblage of dinoflagellates in addition to the two newly determined sequences of *Parvodinium cunningtonii* var. *cunningtonii* (GenBank accession ON980538) and *P. cunningtonii* var. *inerme* (GenBank accession ON980539). Fig. 13 shows 12 strains of *Parvodinium* (three of them referred as ‘*Peridinium*’ as in the original articles where they were sequenced) forming a monophyletic clade with high support from posterior probability (PP = 0.99) and moderate support from bootstrap (BS = 78 %). The two strains of *P. cunningtonii* were sister taxa with maximum support. Together they formed a sister group to a clade that included *Parvodinium parvulum*, *P. elpatiewskyi* (Ostenfeld) Kretschmann, Zerdoner & Gottschling, *P. mixtum* Kretschmann, Owsiany, Zerdoner & Gottschling, ‘*P. inconspicuum*’ and one unidentified strain. The support for this branching pattern was PP = 1.0 and BS = 90 %. The earliest diverging lineage within *Parvodinium* consisted of ‘*Peridinium umbonatum* var. *inaequale*’, ‘*P. centenniale*’ and two strains with uncertain identity. Following the

Fig. 9. *Parvodinium cunningtonii* var. *inerme* var. nov., flagellar apparatus and peduncle, TEM. Continuation of series from Fig. 8. Slanted numbers indicate the section number. (A) A small peduncle (Pe) surrounded by the peduncle striated collar (PSC) is extruded; the microtubules forming the Pe are marked by arrows. The longitudinal microtubular root (LMR/r1), the single-stranded microtubular root (SMR/r2) and the transverse striated root microtubule (TSRM/r4) are still visible. TMRE/r3E, transverse microtubular root extension; TFC, transverse flagellar canal; LFC, longitudinal flagellar canal. (B, C) The TMRE/r3E curves and extends to the dorsal side of the cell. Note the pusular tube (pu) that emerges from the TFC. Scale bars: 500 nm; (B, C) to the same scale.



LSU rDNA-based phylogeny the closest sister lineage to *Parvodinium* encompassed *Palatinus* spp., *Peridiniopsis borgei* and *Johsia chumphonensis*. However, this branching pattern was not well supported (PP = 0.78 and BS < 50 %). As is typical for gene trees based on LSU rDNA sequences the backbone of dinoflagellates lineages was unresolved (polytomy) leaving us with no possibility to infer their evolutionary history.

In the concatenated analysis which only comprised the most closely related dinoflagellate lineages based on the LSU rDNA data matrix, both BA and RaxML suggested *Parvodinium* to be monophyletic (PP = 0.98 and BS = 77 %). With respect to *Parvodinium cunningtonii* var. *inermis* (GenBank accession ON980537) it branched off as the second deepest lineage among *Parvodinium* spp. and thus formed a sister taxon to most species except '*Parvodinium* cf. *umbonatum*' (Fig. 14). The phylogenetic position of *P. cunningtonii* var. *inermis* also received high branch support (PP = 1.0 and BS = 99 %). Furthermore, the branch length to *P. cunningtonii* var. *inermis* was relatively long indicating that the species was genetically distinct. Contrary, the branch lengths (genetic distances) between congeners (*P. parvulum*, *P. elpatiewskyi*, *P. mixtum* and *P. trawinskii*) were comparatively short.

Discussion

Identity and phylogenetic affinities

The general morphology, plate arrangement and spine distribution of the culture line designated above as 'strain 2'/*P. cunningtonii* identifies it as *Peridiniopsis cunningtonii*, as described by Lemmermann in West (1907) from the African Lake Tanganyika and represented in freshwater dinoflagellate floras (Lefèvre 1932, as *Peridinium cunningtonii* (Lemmermann) Lemmermann; Moestrup and Calado 2018; Popovský and Pfister 1990). The epithecal tabulation observed in cells of this strain corresponds to the one described for *Peridinium cunningtonii* var. *pseudoquadridens* Er. Lindemann (1919). We follow Lefèvre (1932),

who regarded this as a tabulation variant, and take Lindemann's variety as a synonym of *Peridiniopsis cunningtonii*, pending further research on these variations (Kretschmann et al. 2019). The presence of spines in the major hypothecal plates, except on plate 3''', agrees with the original drawings and description, and with several later representations of the species (West 1907; Lindemann 1919, as *Peridinium cunningtonii* var. *pseudoquadridens*; Bourrelly 1970; Couté and Iltis 1984; Hansen and Flaim 2007).

The absence of spines in the hypotheca of cells of the population from which strain 1 originated, and the constancy of this feature in culture, would impede the morphological identification of this material as typical *P. cunningtonii*, despite the similarity in epithecal tabulation of the two strains. The variations in the position of plate 1a (contacting the apical pore in a few of the cells examined) seen in strain 1 further suggest that such tabulation variants carry a reduced taxonomic signal. The very small genetic distance found between the two strains studied herein indicates close relatedness, and we therefore describe strain 1 as a variety within the same species. The new variety is distinguished from other varieties of *Peridiniopsis cunningtonii* recognized in Moestrup and Calado (2018) – *P. cunningtonii* var. *excavata* (M. Lefèvre) Moestrup and *P. cunningtonii* var. *treubii* (Włoszyńska) Moestrup – by the pointed antapex and the absence of hypothecal spines.

The LSU rDNA-based phylogeny resolved the two strains herein reported on as sister taxa. Both this and the concatenated phylogeny placed the species in a clade that includes species of *Parvodinium*, whereas the type of *Peridiniopsis* appeared in a different clade together with the genera *Johsia* and *Palatinus*. The corresponding transfer to the genus *Parvodinium* of *P. cunningtonii* is effected below (see Taxonomic summary).

Cyst and cell division

The cyst produced by *Parvodinium cunningtonii* var. *inermis* is smooth-walled, with the same shape of the swimming cell, similarly to what was found in species of the

Fig. 10. *Parvodinium cunningtonii* var. *cunningtonii*, flagellar apparatus and peduncle, TEM. Non-adjacent serial sections progressing from the apex to the antapex of a cell slightly tilted to the right. Slanted numbers indicate the section number. (A–D) The transverse microtubular root extension (TMRE/r3E), sectioned after its curvature, and two rows of the microtubular strand of the peduncle (MSP) accompanied by vesicles (black arrows) are visible. A pusular tube (pu) extends from the transverse flagellar canal (TFC) to the dorsal side of the cell. The transverse striated root (TSR), with its associated transverse striated root microtubule (TSRM/r4), and the transverse microtubular root (TMR/r3) are seen approaching the transverse basal body (TB). Note the different aspect of the platelets (pl), that form the exiting canal of the transverse flagellum, from the outer thecal plates (double arrowheads). (E, F) The longitudinal microtubular root (LMR/r1) and the single-stranded microtubular root (SMR/r2) are seen joining the longitudinal basal body (LB). Electron-opaque material covers the dorsal side of the LMR/r1 (white arrows). (G, H) The peduncle (Pe), surrounded by the peduncle striated collar (PSC) at its base, extrudes through a narrow canal made by platelets (pl). The longitudinal flagellar canal (LFC) extends into the pusular vesicle (puv) that includes granulated bodies (arrowheads). Double arrowheads indicate the outer thecal plates. TSC, transverse striated collar; LSC, longitudinal striated collar. All to the same scale. Scale bar: 500 nm.

P. umbonatum–inconspicuum complex (Chu et al. 2008; Tardio et al. 2009; Wall et al. 1973). Spherical to ovoid cysts with smooth wall have been described from several *Parvodinium* species, e.g., *P. marciniakii*, *P. mixtum*, *P. elpatiewskyi* (Kretschmann et al. 2018, 2019) as well as from *P. cunningtonii* (Lemmermann 1910; Sako et al. 1984). The spherical cyst described for *P. cunningtonii* by Sako et al. (1984) resulted from transformation of a sexually produced planozygote. However, sexual reproduction was not detected in our cultures.

Cell division in Peridinales commonly occurs after the cell stops swimming and two daughter cells form inside the old amphiesma, from which the cells emerge, in most cases, completely separated (Fensome et al. 1993; Moestrup and Calado 2018). Although complete separation of daughter cells was never observed in *P. cunningtonii* var. *inerme*, it is noteworthy that the process leading to cell division in this taxon somewhat resembles the one described from some members of the Peridiniopsidaceae, such as *Palatinus apiculatus* and ‘*Scrippsiella*’ *hexapraeacungula*. In the latter two taxa, an incompletely divided daughter cell exits the parental amphiesma and remains swimming for some time in this semi-divided stage before completing division (Craveiro et al. 2009; Horiguchi and Chihara 1983; West 1909). The formation of thecal plates in the incompletely divided stage, which resulted in a compound theca, was described by Lindemann (1919, as *Peridinium cunningtonii* var. *pseudoquadridens*).

General fine structure and apical pore complex

The general fine-structural features of *Parvodinium cunningtonii* and var. *inerme* are the typical for photosynthetic dinoflagellates with an apical pore, including: a nucleus with condensed chromosomes; chloroplast lobes with thylakoids arranged in groups of three; a pusular system; trichocysts, oil droplets and starch grains scattered in the cytoplasm; and a complex of fibres associated with the apical pore. This complex of fibres resembles the apical pore complex recently described from a strain of the *Parvodinium umbonatum–inconspicuum* complex and those of several other peridinioids with an apical pore, e.g. *Scripp-*

siella sweeneyae Balech, *Peridiniopsis borgei*, *Chimonodinium lomnickii* (Wołoszyska) Craveiro, Calado, Daugbjerg, Gert Hansen & Moestrup and *Theleodinium calcisporum* Craveiro, Pandeirada, Daugbjerg, Moestrup & Calado (Calado and Moestrup 2002; Craveiro et al. 2011, 2013; Roberts et al. 1987). Although the aspect of the apical fibrous complex depends upon the fixation method used (here shown from material fixed with a mixture containing osmium tetroxide), the basic arrangement of a fibrous cylinder that lines the inside of the pore plate and extends posteriorly into several peripheral fibres seems to be common to all these species (Pandeirada et al. 2022; Roberts et al. 1987).

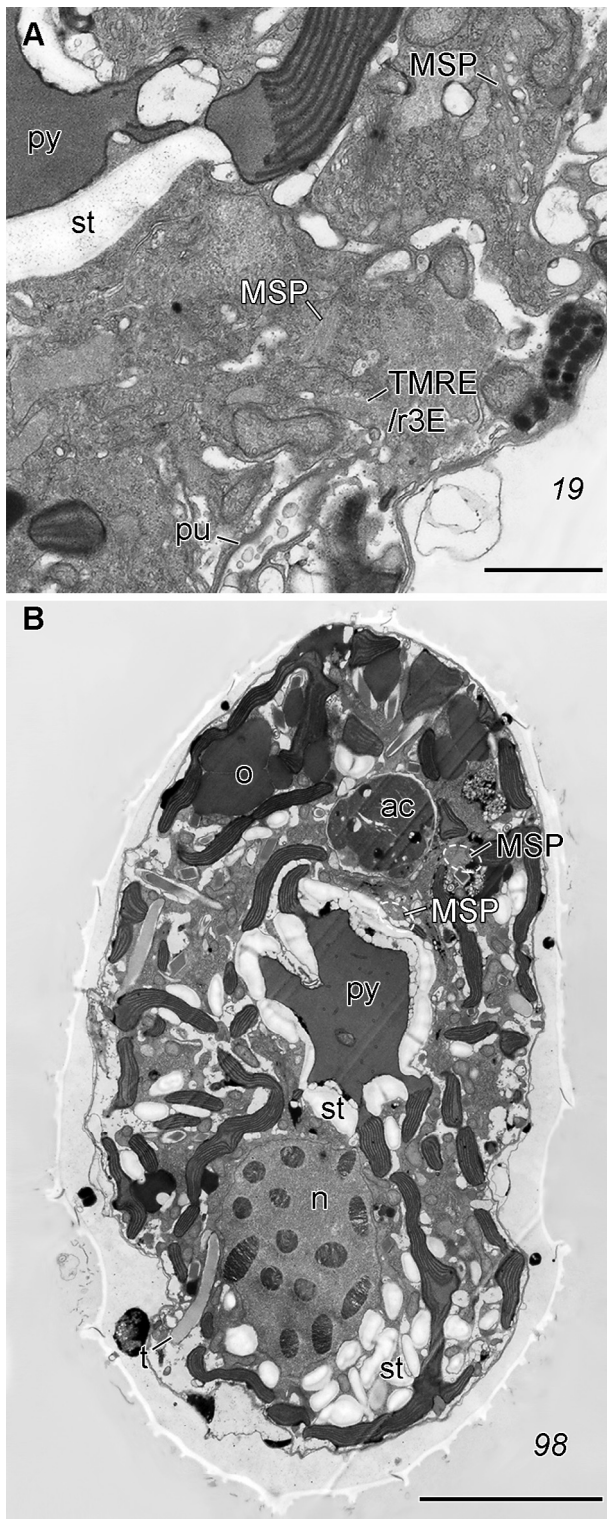
The presence in both strains of *P. cunningtonii* of a pyrenoid surrounded by a starch sheath in the middle of the epicone, from which the chloroplast lobes extend to the periphery, differs from what was found in *Parvodinium umbonatum–inconspicuum* and in *P. parvulum*, but resembles that found in *Peridiniopsis borgei* and *Johsia chumphonensis* (Calado and Moestrup 2002; Luo et al. 2020; Pandeirada et al. 2022). The presence of numerous cytoplasmic channels of irregular shape within the pyrenoid matrix is a relatively uncommon feature shared with *Palatinus apiculatus*, in which the central pyrenoid differs from that of *P. cunningtonii* in being somewhat stellate and by lacking a starch sheath (Craveiro et al. 2009). A pyrenoid penetrated by cytoplasmic channels is also present in *Bysmatrum arenicola* T. Horiguchi & Pienaar (Horiguchi and Pienaar 1988, as ‘*Scrippsiella arenicola*’ nom. inval.) and in species of *Heterocapsa*, two genera distantly related to the Peridiniopsidaceae (Tamura et al. 2005; Tillmann et al. 2017).

The eyespot in both strains of *P. cunningtonii* is of type A, as observed in all *Parvodinium* species for which ultrastructural features are known (Luo et al. 2020; Pandeirada et al. 2022).

Pusule and flagellar apparatus

Long, well-defined pusular tubes were found associated with the transverse flagellar canal (TFC) in *Palatinus apiculatus* (two tubes) and in *Parvodinium umbonatum–incon-*

Fig. 11. *Parvodinium cunningtonii* var. *cunningtonii*, flagellar apparatus and microtubular strand of the peduncle (MSP), TEM. Non-adjacent longitudinal serial sections proceeding toward the left side of the cell, view from the right side. Slanted numbers indicate the section number. (A) General view of the cell showing the position of the nucleus (n) with one nucleolus (nu), the pyrenoid (py) surrounded by starch (st), the somewhat retracted ventral region with the transverse basal body (TB) and the position of the microtubular strand of the peduncle (MSP). (B) The transverse basal body (TB) connects to the proximal-dorsal side of the longitudinal microtubular root (LMR/r1) through two short fibres (two arrows). The layered connective (LC) is between the electron-opaque material (white arrows) on the dorsal side of the LMR/r1 and the TB. The microtubular strand of the peduncle (MSP, black letters) extends to the anterior side of the cell. (C–E) The transverse microtubular root extension (TMRE/r3E) shows its curving path around the anterior side of the transverse flagellar canal (TFC). Note the ascending path of the MSP (black letters) in the ventral side of the cell and the descending path of the MSP (white letters) to the dorsal side. LMR/r1, longitudinal microtubular root; TMR/r3, transverse microtubular root; PSC, peduncular striated collar. Scale bars: 5 μ m (A); 1 μ m (C); 500 nm (B, D, E).



spicum (one tube) but are absent in *Peridiniopsis borgei* (Calado and Moestrup 2002; Craveiro et al. 2009; Pandeirada et al. 2022). *Parvodinium cunningtonii* var. *cunningtonii* and *P. cunningtonii* var. *inermis* also showed one pusular tube connected to the TFC, which branched distally and was internally lined by electron-opaque granules in some portions of its extension. This part of the pusular apparatus is reminiscent of the one found in *Parvodinium umbonatum–inconspicuum* (Pandeirada et al. 2022). *Peridiniopsis borgei* and *Palatinus apiculatus* have a sac pusule associated with the longitudinal flagellar canal (LFC), in contrast to *P. umbonatum–inconspicuum* and *P. cunningtonii*, which lack a sac pusule; instead, there is in the former a complex system that includes a flat vesicle that ramifies into tubular portions, and a complex network of tubes; and in the latter, a simple flat pusular vesicle with several ramifications (Pandeirada et al. 2022; present work). Despite their complexity, which makes them difficult to compare, the pusular systems so far described from *Parvodinium* species seem to display more affinities with one another than with the pusular arrangements described from other Peridiniopsidaceae (particularly *Peridiniopsis borgei* and *Palatinus apiculatus*).

In general, the flagellar apparatus of the two varieties of *Parvodinium cunningtonii* is similar to that recently described from *Parvodinium umbonatum–inconspicuum*. The differences that stand out are mainly quantitative, particularly in the number of microtubules in the TMRE/r3E (one row of ca. 22 in *P. cunningtonii* and one row of ca. 11 in *P. umbonatum–inconspicuum*) and in the path they describe (Pandeirada et al. 2022). In *P. umbonatum–inconspicuum* the TMRE/r3E is relatively short and extends to the dorsal-left side of the cell, over the TFC, whereas in *P. cunningtonii* the path is longer and more complex, with the TMRE/r3E curving around the anterior edge of the TFC and continuing in a posterior direction until it turns and extends to the dorsal side of the cell. Among the species of Peridiniopsidaceae so far examined in detail, the TMRE/r3E of *Peridiniopsis borgei* is the most distinct, with 23 microtubules branching off from a larger microtubular strand to make a cylindrical arrangement around an axial fibre; the arrangement is stable along a path of over

Fig. 12. *Parvodinium cunningtonii* var. *cunningtonii*, microtubular strand of the peduncle (MSP) and transverse microtubular root extension (TMRE/r3E), TEM. Continuation of series of sections from Fig. 11. Slanted numbers indicate the section number. (A) The position of the MSP is indicated in the ascending path (black letters) on the ventral side of the pyrenoid (py) and on the descending path (white letters) passing near the TMRE/r3E. (B) Longitudinal section showing the relative position of the MSP on the ascending path, near the accumulation body (ac), and also in the descending path on the anterior-ventral side of the pyrenoid. n, nucleus; o, oil globule; pu, pusule; st, starch grains; t, trichocyst. Scale bars: 1 μm (A); 1 μm (D); 500 nm (B, C, E).

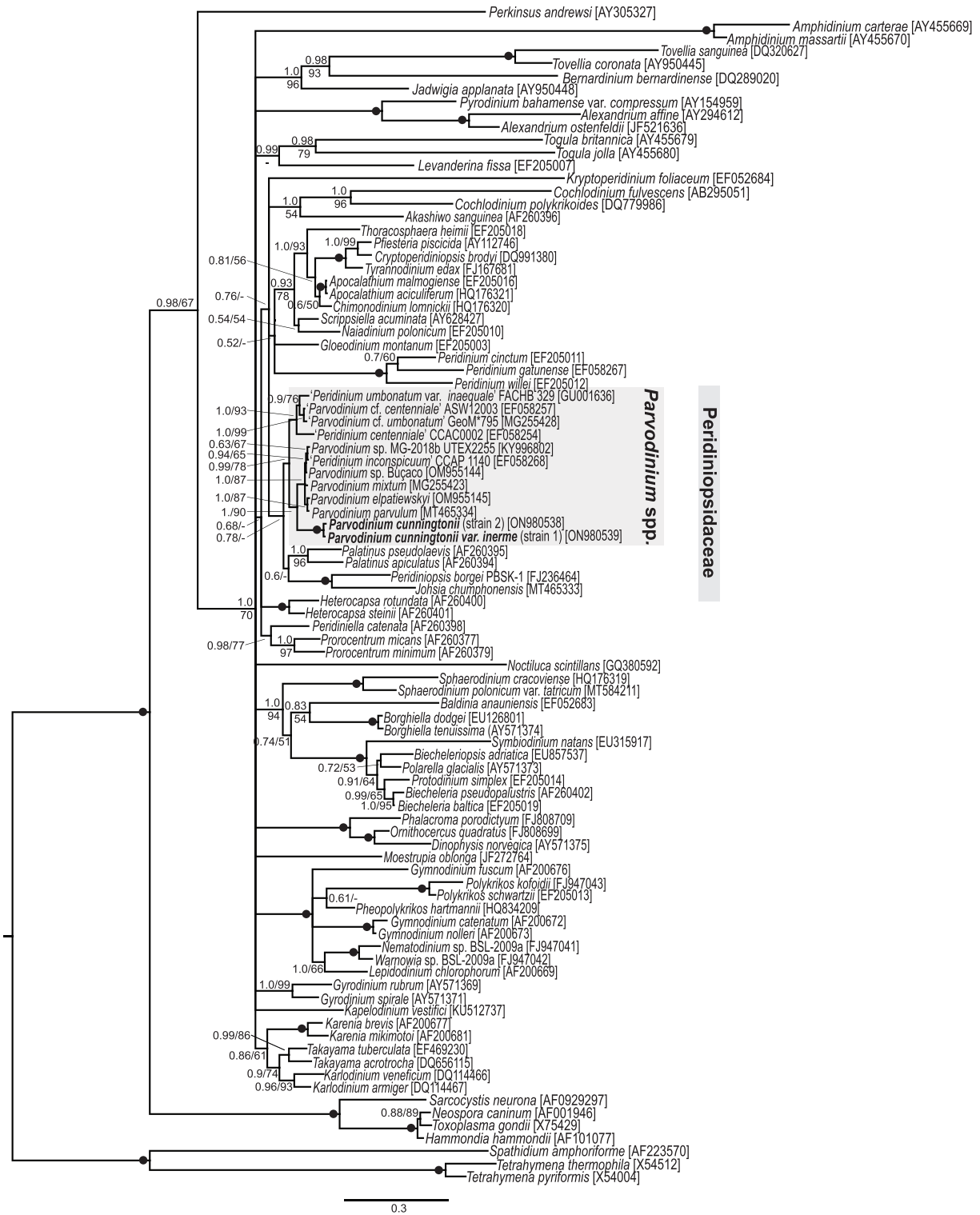


Fig. 13. Phylogeny of *Parvodinium cunningtonii* var. *cunningtonii* and *P. cunningtonii* var. *inerme* based on nuclear-encoded partial LSU rDNA (1,635 base pairs, including introduced gaps). The phylogeny was inferred from Bayesian analysis (BA) and included a diverse assemblage of dinoflagellates (83 sequences and 52 genera). Ciliates, apicomplexans and *Perkinsus* formed the outgroup. Robustness of the tree topology (branch support) was obtained from posterior probabilities (PP ≥ 0.5 ; BA) and bootstrap (BS ≥ 50 %; 1,000 replications in RAxML). The values are written at internodes. PP < 0.5 and BS < 50 % are denoted by a dash (-). Filled circles indicate the highest possible support: 1.0 in BA and 100 % in BS. GenBank accession numbers follow the names of species. The branch lengths are proportional to the number of character changes, see scale bar.

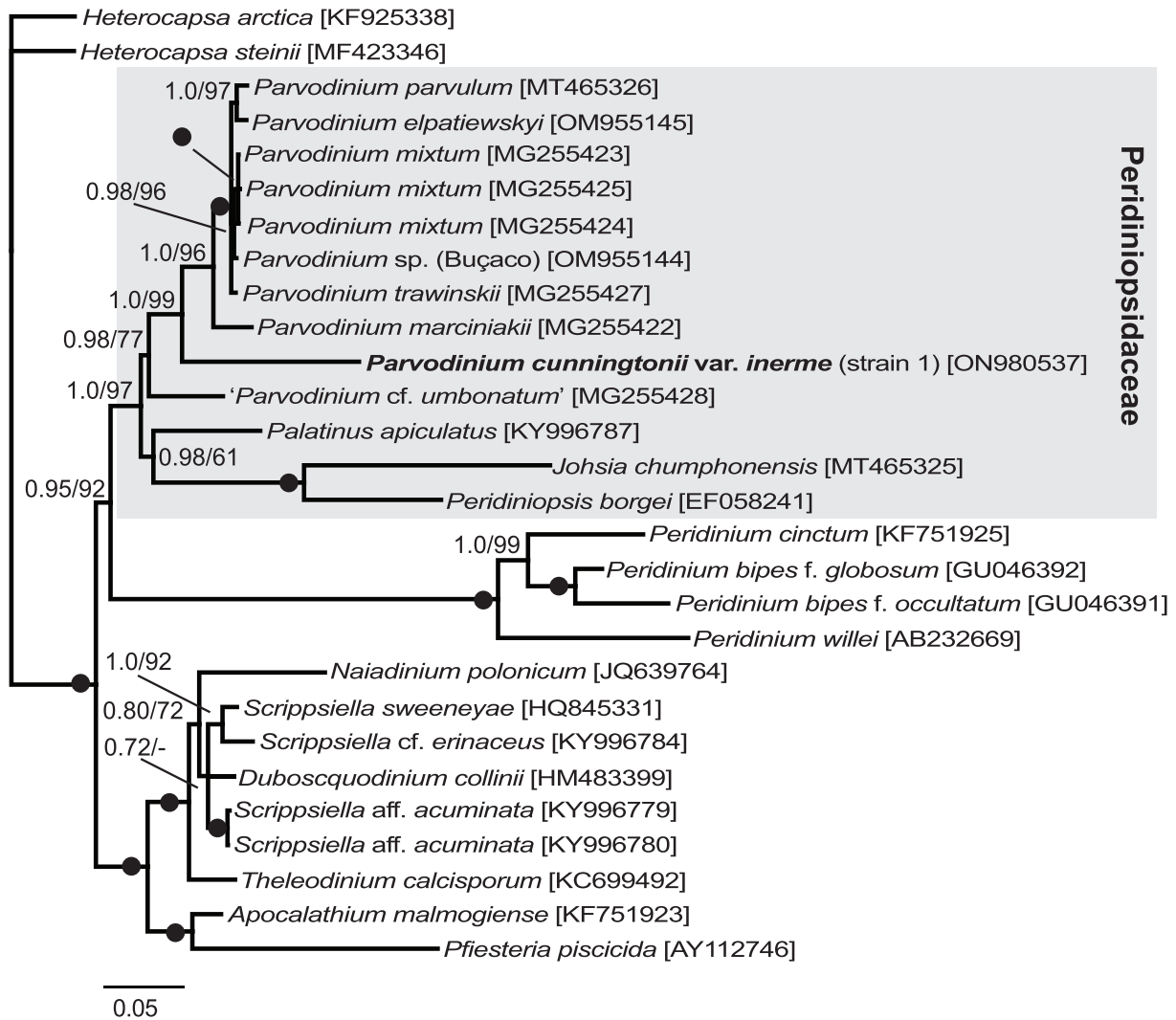


Fig. 14. Phylogeny of *Parvodinium cunningtonii* var. *inerme* based on concatenation of SSU rDNA, ITS 1, 5.8S rDNA, ITS 2 and partial LSU rDNA totaling 3,923 base pairs. The phylogeny was inferred from Bayesian analysis (BA) and included 27 other dinoflagellate sequences of which 10 belonged to *Parvodinium* spp. *Heterocapsa* spp. formed the outgroup. Robustness of the tree topology (branch support) was obtained from posterior probabilities (PP ≥ 0.5 ; BA) and bootstrap (BS $\geq 50\%$; 1,000 replications in RAxML). The values are written at internodes. PP < 0.5 and BS $< 50\%$ are denoted by a dash (-). Filled circles indicate the highest possible support: 1.0 in BA and 100% in BS. GenBank accession numbers follow the names of species. The branch lengths are proportional to the number of character changes, see scale bar.

10 μm around a large sac pusule, toward the dorsally located pyrenoid (Calado and Moestrup 2002). The TMRE/r3E of *Palatinus apiculatus* is much simpler, consisting of one or two strands of microtubules that curve around the ventral and the anterior surfaces of the TFC (Craveiro et al. 2009). Features like the angle and relative position of basal bodies, the four microtubule-containing roots and the layered connective linking LMR/r1 to TSR and TB (and the absence of a longer connective between these two roots) do not seem to provide distinctive characters between the genera of Peridiniopsidaceae. In addition, a two- or three-armed fibrous connective between LMR/r1 and triplets of the TB seems to be shared by members of the Peridiniopsidaceae (see Pandeirada et al. 2022).

Peduncle and microtubular strand of the peduncle

In dinoflagellates, a cytoplasmic extension protruding from the ventral surface, near the insertion area of the flagella (commonly referred to as a peduncle, or sometimes a feeding tube, or a pallium), is usually supported internally by a microtubular strand (MSP) or a microtubular basket (MB) (Calado and Moestrup 1997, 2002). Although the use of the peduncle, feeding tube or pallium for feeding is well documented (e.g., Calado et al. 1998; Calado and Moestrup 1997; reviewed in Hansen and Calado 1999) no unequivocal evidence of the use of extracellular organic particles as food by species of Peridiniopsidaceae is available, and the use of MSP and peduncle in the group is

uncertain. In spite of this, an extruded peduncle has been found in several species of Peridiniopsidaceae. Whereas in *P. cunningtonii* and *Peridiniopsis borgei* an extruded peduncle was detected only in TEM sections, in *P. umbonatum–inconspicuum* it was also visible in SEM (Pandeirada et al. 2022). The path of the MSP inside the cell is rather extensive and complex in all these *Parvodinium* strains and is reminiscent of what was described for *P. borgei*, which has however a larger number of microtubules (ca. 80) (Calado and Moestrup 2002; Pandeirada et al. 2022). Electron-opaque bodies have typically been associated with all types of microtubular apparatuses known to be involved in supporting, or driving, food-uptaking peduncles, feeding tubes and palliums, whether large or small (Calado et al. 1998; Calado and Moestrup 1997; Jacobsen and Anderson 1992). Electron-opaque bodies, and sometimes also electron-translucent elongated vesicles, have also been found in association with the MSP or MB in several photosynthetic dinoflagellates not known to feed on organic particles (e.g., *P. borgei* and *Naiadinium polonicum* (Wołoszyska) Carty, respectively; Calado and Moestrup 2002; Craveiro et al. 2015). The absence of the electron-opaque bodies in *Parvodinium cunningtonii* contrasts with the observation of electron-opaque vesicles in the extruded peduncle of *P. umbonatum–inconspicuum* (Pandeirada et al. 2022). *Palatinus apiculatus* is so far the only member of the Peridiniopsidaceae examined in fine-structural detail that did not show a peduncle and has a relatively small MSP without associated vesicles (Craveiro et al. 2009). Whether these differences reflect different stages in a progressive loss of feeding-related characters inherited from a heterotrophic or mixotrophic ancestor is not clear.

The addition of *P. cunningtonii* to the family Peridiniopsidaceae adds variation in two series of plates to the previously known range of epithecal tabulations: the variants 4', 1a and 5' in the apical region, and six precingular plates (rather than seven) on the base of the epitheca. This underlines the unreliability of tabulation formulas for establishing a classification, and the uncertainty about the phylogenetic affinities of other taxa currently classified as *Peridiniopsis* or *Parvodinium* and not yet analysed by modern methods.

Taxonomic summary

Meeting the requirements of the ICN 2018 (Turland et al. 2018).

Parvodinium cunningtonii (Lemmermann) Pandeirada, Craveiro, Daugbjerg, Moestrup and Calado comb. nov.

Basionym: *Peridiniopsis cunningtonii* Lemmermann in West 1907, J. Linn. Soc., Bot. 38, p. 189, pl. 9, fig. 2.

Homotypic synonym: *Peridinium cunningtonii* (Lemmermann) Lemmermann 1910, p. 671.

Parvodinium cunningtonii var. *inerme* Pandeirada, Craveiro, Daugbjerg, Moestrup and Calado var. nov.

Diagnosis: Differs from *Parvodinium cunningtonii* var. *cunningtonii* in the shape of the hypocone, which tapers into an antapical apiculum, and by lacking spines in the hypotheca; the amphiesmal plates are generally smooth; cells, on average, slightly smaller than the typical variety, mostly 18–30 µm long, 12–21 µm wide and 13–16 µm thick. The genetic distance from the strain of *P. cunningtonii* var. *cunningtonii* described herein is 0.0032, representing four substitutions out of 1260 base pairs of the nuclear-encoded LSU rDNA.

Holotype: SEM stub with critical-point-dried cells from a culture batch, fixed in ethanol 25 % (final concentration). Deposited at the University of Aveiro Herbarium, registered as AVE-A-T-15. Fig. 2B, C illustrate cells from this stub. GenBank accession ON980537.

Type locality: Flooded area of the freshwater stream Ribeiro da Palha near the village of Nariz, Aveiro, Portugal (40°33.240'N, 8°34.095'W), collected 16 July 2015 by M. Pandeirada.

Etymology: Infrspecific epithet from Latin *inermis*, -e, unarmed, without spines or prickles.

CRedit authorship contribution statement

Mariana S. Pandeirada: Investigation, Writing – original draft, Visualization. **Sandra C. Craveiro:** Resources, Writing – review & editing, Visualization. **Niels Daugbjerg:** Formal analysis, Writing – review & editing. **Øjvind Moestrup:** Resources, Writing – review & editing. **António J. Calado:** Conceptualization, Writing – review & editing, Supervision.

Declaration of Competing Interest

The authors declare that they have no known competing financial interests or personal relationships that could have appeared to influence the work reported in this paper.

Acknowledgments

To the Laboratory of Molecular Studies for Marine Environments (LEMAM), Univ. Aveiro, Portugal, where the molecular work was conducted by M.S.P. and S.C.C.

Funding

M.S.P. was supported by the grant SFRH/BD/109016/2015, from the financing program POCH (Programa Operacional Capital Humano), the European Social Funding (FSE) and the Portuguese Ministry of Science, Technology and Higher Education (MCTES). Additional

support came from the GeoBioTec Research Unit (UID/GEO/04035/2019), and from national funds (OE), to S.C. C., through FCT – “Fundação para a Ciência e a Tecnologia”, I.P., in the scope of the framework contract foreseen in the numbers 4, 5 and 6 of the article 23 of the Decree-Law 57/2016, of 29 August, changed by Law 57/2017, of 19 July.

References

- Bourrelly, P., 1970. Les algues d'eau douce 3: les algues bleues et rouges, les Eugléniens. Peridiniens et Cryptomonadines, Boubée, Paris, p. 512.
- Calado, A.J., Moestrup, Ø., 1997. Feeding in *Peridiniopsis berolinensis* (Dinophyceae): new observations on tube feeding by an omnivorous, heterotrophic dinoflagellate. *Phycologia* 36 (1), 47–59.
- Calado, A.J., Moestrup, Ø., 2002. Ultrastructural study of the type species of *Peridiniopsis*, *Peridiniopsis borgei* (Dinophyceae), with special reference to the peduncle and flagellar apparatus. *Phycologia* 41, 567–584.
- Calado, A.J., Craveiro, S.C., Moestrup, Ø., 1998. Taxonomy and ultrastructure of a freshwater, heterotrophic *Amphidinium* (Dinophyceae) that feeds on unicellular protists. *J. Phycol.* 34, 536–554.
- Carty, S., 2008. *Parvodinium* gen. nov. for the Umbonatum group of *Peridinium* (Dinophyceae). *Ohio J. Sci.* 108, 103–107.
- Chu, G., Sun, Q., Rioual, P., Boltovskoy, A., Liu, Q., Sun, P., Han, J., Liu, J., 2008. Distinct microlaminations and freshwater “red tides” recorded in Lake Xiaolongwan, northeastern China. *J. Paleolimnol.* 39, 319–333.
- Couté, A., Iltis, A., 1984. Mise au point sur la flore péridiniale (Algae, Pyrrhophyta) d'eau douce de Côte d'Ivoire. *Rev. Hydrobiol. Trop.* 17, 53–64.
- Craveiro, S.C., Calado, A.J., Daugbjerg, N., Moestrup, Ø., 2009. Ultrastructure and LSU rDNA-based revision of *Peridinium* group palatinum (Dinophyceae) with the description of *Palatinus* gen. nov. *J. Phycol.* 45, 1175–1194.
- Craveiro, S.C., Calado, A.J., Daugbjerg, N., Hansen, G., Moestrup, Ø., 2011. Ultrastructure and LSU rDNA-based phylogeny of *Peridinium lomnickii* and description of *Chimonodinium* gen. nov. (Dinophyceae). *Protist* 162, 590–615.
- Craveiro, S.C., Pandeirada, M.S., Daugbjerg, N., Moestrup, Ø., Calado, A.J., 2013. Ultrastructure and phylogeny of *Theleodinium calcisporum* gen. et sp. nov., a freshwater dinoflagellate that produces calcareous cysts. *Phycologia* 52, 488–507.
- Craveiro, S.C., Daugbjerg, N., Moestrup, Ø., Calado, A.J., 2015. Fine-structural characterization and phylogeny of *Peridinium polonicum*, type species of the recently described genus *Naiadinium* (Dinophyceae). *Eur. J. Protistol.* 51, 259–279.
- Daugbjerg, N., Hansen, G., Larsen, J., Moestrup, Ø., 2000. Phylogeny of some of the major genera of dinoflagellates based on ultrastructure and partial LSU rDNA sequence data, including the erection of three new genera of naked dinoflagellates. *Phycologia* 39, 302–317.
- Fensome, R.A., Taylor, F.J.R., Norris, G., Sarjeant, W.A.S., Wharton, D.I., Williams, G.L., 1993. A classification of living and fossil dinoflagellates. *Micropaleontology, Special Publication* 7, 1–351.
- Gottschling, M., Kretschmann, J., Žerdoner alasan, A., 2017. Description of Peridiniopsidaceae, fam. nov. (Peridinales, Dinophyceae). *Phytotaxa* 299, 293–296.
- Hansen, G., Daugbjerg, N., 2004. Ultrastructure of *Gyrodinium spirale*, the type species of *Gyrodinium* (Dinophyceae), including a phylogeny of *G. dominans*, *G. rubrum* and *G. spirale* deduced from partial LSU rDNA sequences. *Protist* 155, 271–294.
- Hansen, G., Flaim, G., 2007. Dinoflagellates of the Trentino Province, Italy. *J. Limnol.* 66, 107–141.
- Horiguchi, T., Chihara, M., 1983. *Scrippsiella hexapraeacungula* sp. nov. (Dinophyceae), a tide pool dinoflagellate from the Northwest Pacific. *Bot. Mag. Tokyo* 96, 351–358.
- Horiguchi, T., Pienaar, R.N., 1988. Ultrastructure of a new sand-dwelling dinoflagellate, *Scrippsiella arenicola* sp. nov.. *J. Phycol.* 24, 426–438.
- Huelsenbeck, J.P., Ronquist, F., 2001. MRBAYES: Bayesian inference of phylogenetic trees. *Bioinformatics* 17 (8), 754–755.
- Jacobson, D.M., Anderson, D.M., 1992. Ultrastructure of the feeding apparatus and myonemal system of the heterotrophic dinoflagellate *Protoperidinium spinulosum*. *J. Phycol.* 28, 69–82.
- Kretschmann, J., Owsianny, P.M., Žerdoner alasan, A., Gottschling, M., 2018. The hot spot in a cold environment: puzzling *Parvodinium* (Peridiniopsidaceae, Peridinales) from the polish Tatra mountains. *Protist* 169, 206–230.
- Kretschmann, J., Žerdoner alasan, A., Meyer, B., Gottschling, M., 2019. Zero intercalary plates in *Parvodinium* (Peridiniopsidaceae, Peridinales) and phylogenetics of *P. elpatiewskyi*, comb. nov. *Protist* 171, 125700.
- Lefe`vre, M., 1932. Monographie des espe`ces d'eau douce du genre *Peridinium* Ehrb. *Arch. Bot. Mém.* 2 (Mémoire 5), 1–210, pls 1–6.
- Lemmermann, E., 1910. Algen I (Schizophyceen, Flagellaten, Peridineen). *Kryptogamenflora der Mark Brandenburg*, Bd. 3, 712.
- Lindemann, E., 1919. Untersuchungen über Süßwasserperidineen und ihre Variationsformen. *Arch. Protistenk.* 39, 209–262, + pl 17.
- Lindström, K., 1991. Nutrient requirements of the dinoflagellate *Peridinium gatunense*. *J. Phycol.* 27, 207–219.
- Luo, Z., Mertens, K.N., Gu, H., Wang, N.a., Wu, Y., Uttayammanee, P., Pransilpa, M., Roeroe, K.A., 2020. Morphology, ultrastructure and molecular phylogeny of *Johsia chumphonensis* gen. et sp. nov. and *Parvodinium parvulum* comb. nov. (Peridiniopsidaceae, Dinophyceae). *Eur. J. Phycol.* 56, 324–336.
- Moestrup, Ø., Calado, A.J., 2018. Dinophyceae. In: Büdel, B., Gärtner, G., Krienitz, L., Schagerl, M. (Eds.), *Süßwasserflora von Mitteleuropa – Freshwater Flora of Central Europe*, vol. 6, 2nd ed. Springer-Verlag, Berlin. XII + 561 pp.
- Nichols, H.W., 1973. Growth media — freshwater. In: Stein, J.R. (Ed.), *Handbook of phycological methods. Culture methods & growth measurements*. Cambridge University Press, Cambridge, pp. 7–24.

- Nunn, G.B., Theisen, B.F., Christensen, B., Arctander, P., 1996. Simplicity-correlated size growth of the nuclear 28S ribosomal RNA D3 expansion segment in the crustacean order Isopoda. *J. Mol. Evol.* 42, 211–223.
- Pandeirada, M.S., Craveiro, S.C., Daugbjerg, N., Moestrup, Ø., Calado, A.J., 2014. Studies on woloszynskioid dinoflagellates VI: description of *Tovellia aveirensis* sp. nov. (Dinophyceae), a new species of Tovelliaceae with spiny cysts. *Eur. J. Phycol.* 49, 230–243.
- Pandeirada, M.S., Craveiro, S.C., Daugbjerg, N., Moestrup, Ø., Calado, A.J., 2017. Studies on woloszynskioid dinoflagellates VIII: life cycle, resting cyst morphology and phylogeny of *Tovellia rinoi* sp. nov. (Dinophyceae). *Phycologia* 56, 533–548.
- Pandeirada, M.S., Craveiro, S.C., Daugbjerg, N., Moestrup, Ø., Calado, A.J., 2022. Cell fine structure and phylogeny of *Parvodinium*: towards an ultrastructural characterization of the Peridiniopsidaceae (Dinophyceae). *Eur. J. Phycol.* <https://doi.org/10.1080/09670262.2022.2091798>, In press.
- Popovský, J., Pfister, L.A., 1990. Dinophyceae (Dinoflagellida). In: Ettl, H., Gerloff, J., Heynig, H., Mollenhauer, D. (Eds.), *Süßwasserflora von Mitteleuropa*, vol. 6. Gustav Fischer, Jena.
- Roberts, K.R., Timpano, P., Montegut, A.E., 1987. The apical fibrous complex: a new cytological feature of some dinoflagellates. *Protoplasma* 137, 65–69.
- Sako, Y., Ishida, Y., Kadota, H., Hata, Y., 1984. Sexual reproduction and cyst formation in the freshwater dinoflagellate *Peridinium cunningtonii*. *NIPPON SUISAN GAKKAISHI* 50 (5), 743–750.
- Scholin, C.A., Herzog, M., Sogin, M., Anderson, D.M., 1994. Identification of group- and strain-specific genetic markers for globally distributed *Alexandrium* (Dinophyceae). II. Sequence analysis of a fragment of the LSU rRNA gene. *J. Phycol.* 30, 999–1011.
- Stamatakis, A., 2014. RAxML version 8: a tool for phylogenetic analysis and post-analysis of large phylogenies. *Bioinformatics* 30, 1312–1313. doi.org/10.1093/bioinformatics/btu033.
- Swofford, D.L., 2002. *Phylogenetic Analysis Using Parsimony (*and other methods)*. Version 4. Sinauer Associates, Sunderland, Massachusetts.
- Takano, Y., Horiguchi, T., 2005. Acquiring scanning electron microscopical, light microscopical and multiple gene sequence data from a single dinoflagellate cell. *J. Phycol.* 42, 251–256.
- Tamura, M., Iwataki, M., Horiguchi, T., 2005. *Heterocapsa psammophila* sp. nov. (Peridinales, Dinophyceae), a new sand-dwelling marine dinoflagellate. *Phycol. Res.* 53, 303–311.
- Tardio, M., Ellegaard, M., Lundholm, N., Sangiorgi, F., Di Giuseppe, D., 2009. A hypocystal archeopyle in a freshwater dinoflagellate from the *Peridinium umbonatum* group (Dinophyceae) from Lake Nero di Cornisello, South-East Alps, Italy. *Eur. J. Phycol.* 44, 1–10.
- Tillmann, U., Hopperath, M., Gottschling, M., Kusber, W., Elbrächter, M., 2017. Plate pattern clarification of the marine dinophyte *Heterocapsa triquetra* sensu Stein (Dinophyceae) collected at Kiel Fjord (Germany). *J. Phycol.* 53, 1305–1324.
- Wall, D., Dale, B., Harada, K., 1973. Descriptions of new fossil dinoflagellates from the Late Quaternary of the Black Sea. *Micropaleontology* 19, 18–31.
- West, G.S., 1909. A biological investigation of the Peridineae of Sutton Park, Warwickshire. *New Phytol.* 8, 181–196.
- West, G.S., 1907. Report on the freshwater algae, including phytoplankton, of the third Tanganyika Expedition conducted by Dr. W.A. Cunningham, 1904–1905. *J. Linn. Soc., Bot.* 38, 81–197. [Class Peridineae studied by E. Lemmermann].